

# **Factors affecting the apparent longitudinal stick-free static stability of a typical high-wing light aeroplane**

**M.A. Bromfield**  
michael.bromfield@brunel.ac.uk

**G.B Gratton**  
guy.gratton@brunel.ac.uk

Brunel Flight Safety Laboratory  
School of Engineering and Design  
Brunel University  
UK

## **ABSTRACT**

Flying a light aeroplane involves a combination of pilot and aeroplane performing a set task, within a specific environment. The pilot is continuously sampling and selecting available sensory cues, interpreting those cues, making decisions and manipulating the primary controls (stick and rudder) to safely achieve flying objectives. The 'feel' of an aeroplane (a flying quality) is directly associated with the stick and rudder forces and how the aeroplane responds to control inputs. Classical theory has been applied to estimate the apparent (as felt by the pilot) longitudinal stick-free static stability (change of stick force with airspeed) of a typical, two-seat, high-wing light aeroplane. The theory has been extended to consider the effects of tail downwash and flap deflection. The results are compared with actual flight tests and show that the method may be used for the initial assessment of longitudinal stick-free static stability and more importantly, tendencies towards neutral or negative stability affecting flight safety.

## NOMENCLATURE

$a$	lift curve slope (/rad)
$a'$	lift curve slope, elevator free (/rad)
$a_e$	elevator effectiveness or change of tail-plane lift coefficient with elevator deflection (/rad)
$A$	coefficient 'A', speed dependent term in stick force estimation
$b_0$	change of elevator hinge moment coefficient with tail-plane setting (/rad)
$b_1$	change of elevator hinge moment coefficient with angle of attack (/rad)
$b_2$	change of elevator hinge moment coefficient with elevator deflection (/rad)
$b_3$	change of elevator hinge moment coefficient with elevator trim tab deflection (/rad)
BCAR	British Civil Airworthiness Requirements
BFSL	Brunel Flight Safety Laboratory
BHP	brake horse power
$\bar{c}$	mean aerodynamic chord of the wing (ft)
$\bar{c}_e$	mean aerodynamic chord of the elevator (ft)
$C$	coefficient 'C', speed independent term in stick force estimation
CAA	United Kingdom Civil Aviation Authority
CAS	calibrated airspeed (kt)
CG	centre of gravity (in)
$C_{he}$	elevator hinge moment coefficient
$C_L$	lift coefficient for the aeroplane
$C_{L\alpha}$	lift coefficient for the aeroplane due to angle of attack
$C_{L_{trim}}$	lift coefficient for the aeroplane at the trim condition
$C_{L\delta_e}$	lift coefficient for the aeroplane due to elevator deflection
$C_{L_{wb}}$	lift coefficient for the wing-body combination
CofA	certificate of airworthiness
CVR	cockpit voice recorder
$C_{m_0}$	zero lift pitching moment coefficient
$det$	matrix determinant, $det = C_{L\alpha} [C_{L\delta_e} (h_n - h_{n_{wb}}) - a_e \bar{V}_H]$
EAS	equivalent airspeed (kt)
FCCM	flight control mechanical characteristics
FDR	flight data recorder
FTE	flight test engineer
GASCo	General Aviation Safety Council
$G$	elevator gearing (rad/ft)
$h$	location of the centre of gravity (%MAC)
$H_e$	elevator hinge moment
$h_n$	stick fixed neutral point, wing-only (%MAC)
$h_H$	horizontal tailplane height above the wing-chord plane (in)
$h_{n_{wb}}$	stick-fixed neutral point, wing/body combination (%MAC)
$h'_n$	stick-free neutral point (%MAC)
$i_h$	horizontal tail incidence angle, relative to wing-body zero lift line(rad)
IAS	indicated airspeed (kt)
ISA	international standard atmosphere
LSS	longitudinal static stability
$l_t$	distance from centre of gravity to horizontal tail aerodynamic centre (ft)
MAC	mean aerodynamic chord
MATLAB	MATrix LABoratory, a numerical computing environment and 4 <sup>th</sup> generation computer programming language
MTOW	maximum take-off weight (lbf)
$P$	elevator stick force applied by the pilot, pull positive (lbf)
PEC	position error correction

$s$	elevator stick displacement, positive rearwards (in)
$S$	wing area (ft <sup>2</sup> )
$S_e$	elevator area (ft <sup>2</sup> )
$S_t$	horizontal tailplane area (ft <sup>2</sup> )
TAS	true airspeed (kt)
TOW	take-off weight (lbf)
$V$	true airspeed (ft/s)
$V_E$	equivalent airspeed (kt)
$V_S$	stall speed (kt)
$V_{SO}$	stall speed in the landing configuration (kt)
$V_{Trim}$	equivalent airspeed at the trim condition (ft/s)
$\bar{V}_H$	tailplane volume coefficient, $\bar{V}_H = \frac{l_t S_t}{\bar{c} S}$
$w$	wing loading (lbf/ft <sup>2</sup> )
$W$	weight (lbf)
W&CG	weight and balance
$\alpha_{T_{trim}}$	effective angle of attack of the horizontal tailplane at the trim condition (rad)
$\alpha_{wb}$	angle of attack of the wing-body combination from the zero lift line (rad)
$\delta_e$	elevator deflection, positive trailing edge down (rad)
$\delta_{e_{trim}}$	elevator deflection at the trim condition (rad)
$\delta_f$	flap deflection, positive trailing edge down (rad)
$\delta_t$	elevator trim tab deflection, positive trailing edge up (rad)
$\delta_{t_{trim}}$	elevator trim tab deflection at the trim condition (rad)
$\varepsilon$	tail downwash angle, positive downwards (rad)
$\frac{d\varepsilon}{d\alpha}$	downwash derivative (partial)
$\rho$	local air density (slug/ft <sup>3</sup> )
$\rho_o$	air density at ISA sea level conditions (slug/ft <sup>3</sup> )

Note – use of units

This paper refers to airspeed in knots, aircraft weights in lbf and control forces in daN since these units are standard in the majority of operating documents for the aircraft under consideration. 1 kt = 0.515 m/s and 1 lbf = 4.448 N or 0.4448 daN (1 daN = 10 N). The units of deca-Newtons (daN) are commonly used in current EASA Certification standards [1],[2].

## 1 INTRODUCTION

The handling quality of a light aircraft involves a unique and dynamic combination of pilot and aeroplane performing a set task within a specific environment. The pilot is continuously selecting available sensory cues, making decisions, and manipulating primary controls (stick and rudder) to safely achieve objectives. The quality and timeliness of sensory cues have a significant effect on both pilot decisions and performance. The 'feel' of an aeroplane is directly associated with the stick and rudder forces felt by the pilots hands and feet and the response of the aeroplane to those control inputs. Whilst the pilot is controlling flightpath and airspeed, both stick force and position may provide cues with respect to airspeed changes and the proximity to stall (providing the aircraft is not re-trimmed). The apparent stick-free longitudinal static stability (or stick force gradient) is a measure of the aeroplane's natural tendency to return to a trim condition in flight as the airspeed is changed and the elevator is free to float whilst the pilot is hands-off.

Certification standards for light aircraft vary across countries, regions and aeroplane categories as shown in Table 1. All standards require the aircraft to show "suitable stability and control feel in any condition normally encountered". When the aeroplane is trimmed in the climb, cruise or landing, "a pull must be required to obtain and maintain speeds below the specified trim speed and a push required to obtain and maintain speeds above the specified trim speed". However, acceptable stick force gradients (stick force versus airspeed) are only defined for European standards CS-22, Sailplanes & Powered Sailplanes [1] and CS-25, Large Aeroplanes [2] together with corresponding FAR-25 [3] in the United States. European standard CS-23 [4] for Normal, Utility, Aerobatic and Commuter Aeroplanes (General Aviation) and United States FAR-23 [5], state only 'perceptible stick force gradient' with the final judgement being left to the subjective opinion of the test pilot during initial certification of the type. Within the UK [6] and US military [7], there are no defined standards for minimum stick force gradients for light, transport or fighter aircraft [8].

**Table 1, Comparison of Longitudinal Static Stability Certification Requirements**

<b>Aeroplane Category</b>	<b>Airworthiness Requirement (Paragraph Numbers)</b>	<b>Minimum Stick Force Gradient</b>	<b>Maximum Trim Speed Band</b>
Microlight	BCAR Section S [9] (143, 161, 173, 175)	Not defined	±10% trim CAS
General Aviation (pre-1992)	BCAR Section K [10] (2-8,2-9,2-10)	Not defined	Not defined
Very Light Aircraft	CS-VLA [11] (143, 145, 161, 173,175)	Not defined	±10% trim CAS
Sailplanes and Powered Sailplanes	CS-22 [1] (143, 145, 161, 171, 173, 175 AMC 22.173 (a))	1 N / 10 km/h (0.031 daN/kt)	Greater of ±15% or ±15 km/h
General Aviation	CS-23 [4] (143, 145, 161, 171, 173, 175)  FAR-23 [5] (143, 145, 153, 161, 171, 173)	Gradient not defined, positive within ranges and in configurations given in para 175.  In general, within 15% of trim at all conditions.	±10% ±7.5% (cruise conditions, commuter category only)
Commercial	CS-25[2] (143, 145, 161, 171, 173, 175, AMC 22.173 (c))  FAR-25 [3] (143, 145, 153, 161, 171, 173)	1 lbf/ 6 kt or 0.167 lbf/kt (0.074 daN/kt)  The average gradient is taken over each half of the speed range between 0.85 and 1.15 V <sub>Trim</sub>	±10% climb, approach and landing, ±7.5% cruise
Military	DEF STAN 00-970 Part 1/5 Section 2, Leaflet 40 [6]  MIL 8785C [7] (3.2.1.1)	Gradient not defined. Force & deflection must be smooth and stable or Force & deflection gradients can be zero if SAS or CAS are available.  Unstable gradients allowable in transonic flight if not objectionable to the pilot.	±15% or 50 kt, whichever is less

## 2 THEORETICAL ESTIMATION OF APPARENT LONGITUDINAL STICK-FREE STATIC STABILITY

### 2.1 Estimation of Stick Force and Gradient

For non-augmented, reversible control systems without the aid of downsprings or bobweights as found in typical light aeroplanes, pitch control forces can be estimated using theory as described by Etkin & Reid [12]. Figure 1, shows a simplified schematic for an elevator control system.

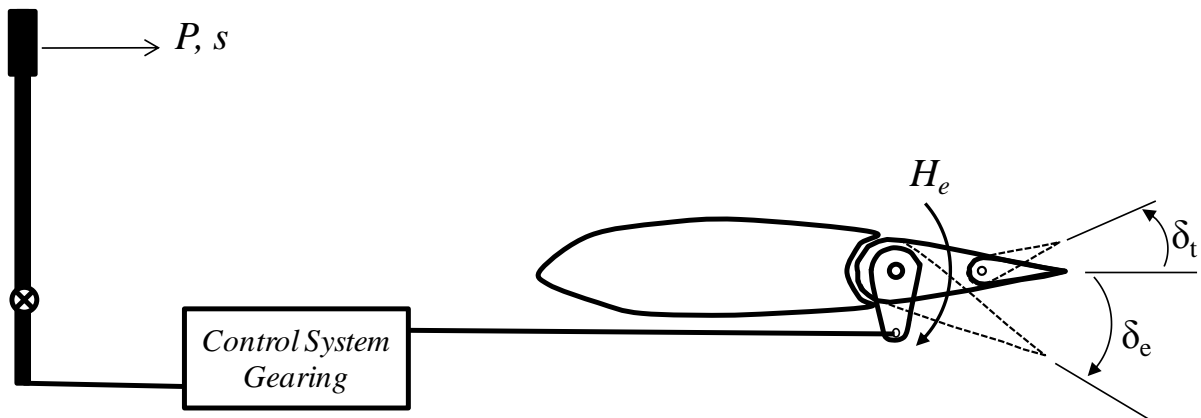


Figure 1, Simplified elevator control system, adapted from Etkin & Reid [12]

The system comprises three main components, the control stick, control system linkage and the elevator. The control system linkage represents the combination of bell cranks, rods, pulleys, cables and turnbuckles commonly found in a typical light aeroplane.

The following assumptions have been made in the application of this classical theory:-

- Flow is incompressible;
- The aeroplane is in a non-stalled condition in cruising flight, with linear (attached) flow;
- Movement outside the OX-OZ plane is ignored i.e. system has 2 degrees of freedom;
- The aeroplane structure is rigid and aero-elastic effects ignored;
- The reversible control system is both mass-less and frictionless;
- No lack of fit at the joints or elasticity in control cables;
- Quasi-static conditions exist;
- Altitude is constant;
- Weight is constant;
- The elevator trim tab is fixed for the initial trim condition;
- The direct and indirect effects of power are ignored.

For a small quasi-static displacement from equilibrium and using conservation of energy gives:-

$$Pds + H_e d\delta_e = 0 \quad \dots(1)$$

Re-arranging,

$$P = -\frac{d\delta_e}{ds} H_e \quad \dots(2)$$

Where:-

$P$  = elevator stick force applied by the pilot (pull positive)  
 $s$  = elevator stick displacement (positive rearwards)

Giving:-

$$P = GH_e \quad \dots(3)$$

Where  $G$  = Elevator Gearing Ratio such that:-

$$G = -\frac{d\delta_e}{ds} > 0 \quad \dots(4)$$

Substituting for the hinge moment coefficient :-

$$H_e = C_{he} S_e \bar{c}_e \frac{1}{2} \rho V^2$$

Gives:-

$$P = GC_{he} S_e \bar{c}_e \frac{1}{2} \rho V^2 \quad \dots(5)$$

This states that the variation of stick force with airspeed depends on both  $V^2$  and how  $C_{he}$  varies with airspeed.

The value of  $C_{he}$  at trim for an arbitrary tab angle is given by:-

$$C_{he} = b_0 + b_1 \alpha_{T_{trim}} + b_2 \delta_{e_{trim}} + b_3 \delta_t \quad \dots(6)$$

Where  $\alpha_{T_{trim}}$ , the effective angle of attack of the tailplane is:-

$$\alpha_{T_{trim}} = \alpha_{wb} + i_t - \varepsilon \quad \dots(7)$$

To fly the aeroplane at a selected  $C_L$  requires a specific elevator deflection angle  $\delta_{e_{trim}}$  but this is balanced by using the elevator trim tab to reduce pilot workload. By re-arranging Equation...(6)  $\delta_{t_{trim}}$  with  $C_{he} = 0$  for the trim condition, we arrive at:-

$$\delta_{t_{trim}} = -\frac{1}{b_3}(b_0 + b_1\alpha_{T_{trim}} + b_2\delta_{e_{trim}}) \quad \dots(8)$$

Combining with the above gives:-

$$C_{he} = b_3(\delta_t - \delta_{t_{trim}}) \quad \dots(9)$$

Etkin & Reid [12] also show that:-

$$\delta_{t_{trim}} = -\frac{1}{b_3} \left[ b_0 + \frac{C_{m_0}}{\det} (b_1 C_{L_{\delta_e}} - b_2 C_{L_\alpha}) - \frac{a'b_2}{\det} (h - h'_n) C_{L_{trim}} \right] \quad \dots(10)$$

Where 'det' is the following determinant:-

$$\det = C_{L_\alpha} \left[ C_{L_{\delta_e}} (h_n - h_{n_{wb}}) - a_e \bar{V}_H \right] \quad \dots(11)$$

and

$h_n$  = stick fixed neutral point (wing only)

$h_{n_{wb}}$  = stick fixed neutral point (wing and body combination)

$$\bar{V}_H = \frac{l_t S_t}{\bar{c} S}$$

Substituting Equation...(10) into Equation...(9), the hinge moment is:-

$$C_{he} = b_3 \delta_t + b_0 + \frac{C_{m_0}}{\det} (b_1 C_{L_{\delta_e}} - b_2 C_{L_\alpha}) - \frac{a'b_2}{\det} (h - h'_n) C_{L_{trim}} \quad \dots(12)$$

For the aeroplane in straight and level flight, lift equals weight, so that:-

$$C_{L_{trim}} = \frac{W}{\frac{1}{2} \rho V^2 S} \quad \dots(13)$$

Or

$$C_{L_{trim}} = \frac{w}{\frac{1}{2}\rho V^2} \quad \dots(14)$$

Where  $w = W/S$ , the wing loading.

Substituting for  $C_{he}$  and  $C_{L_{trim}}$  in equation 4, the simplified result obtained is:-

$$P = C + AV_E^2 \quad \dots(15)$$

In the form of a 2<sup>nd</sup> order polynomial in  $V_E$ , where:-

$$C = GS_e \bar{c}_e w \frac{a' b_2}{\det} (h - h'_n) \quad \dots(16)$$

$$A = \frac{1}{2} \rho_o GS_e \bar{c}_e \left[ b_3 \delta_t + b_0 + \frac{C_{m0}}{\det} (b_1 C_{L_{\delta_e}} - b_2 C_{L_{\alpha}}) \right] \quad \dots(17)$$

and substituting for  $V$  using:-

$$V = V_E \sqrt{\frac{\rho_o}{\rho}} \quad \dots(18)$$

A typical theoretical plot of stick force ( $P$ ) versus airspeed ( $V_E$ ) is shown in Figure 2. Also known the apparent (as felt by the pilot at the aeroplane controls) longitudinal stick-free stability' [13], this is a measure of the aeroplane's natural tendency to return to a trim condition in flight as the airspeed is changed and the elevator is free to float whilst the pilot is hands-off.

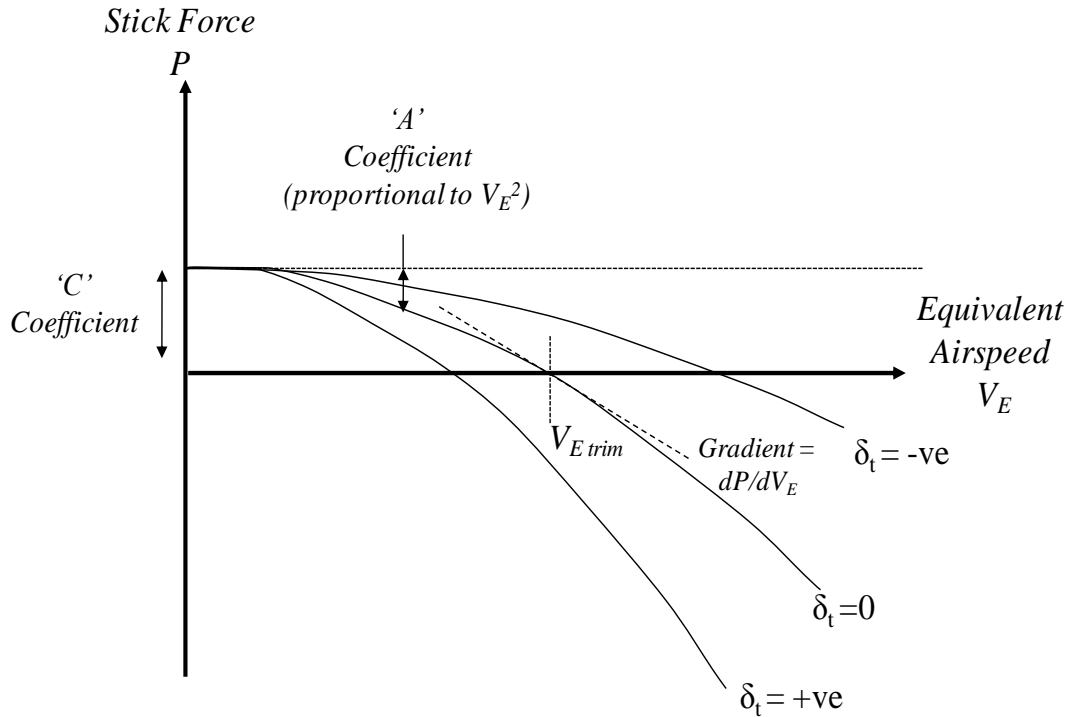


Figure 2, Typical plot of Stick Force versus Airspeed, adapted from [12]

The estimation of stick force gradient, away from the trim condition is given by differentiating Equation ...(15) with respect to  $V_E$  as follows:-

$$\frac{dP}{dV_E} = 2AV_E \quad \dots(19)$$

Inspection of Equation...(16) suggests that the coefficient 'C' is dependent upon CG (via the term for static margin), wing loading (via the term  $w$ ) and elevator gearing (via the gearing term  $G$ ). Inspection of Equation...(17) suggests that the coefficient 'A' is dependent upon trim tab setting (via the  $\delta_t$  term); elevator gearing (via the gearing term  $G$ ). In summary:-

$$C = f(h - h'_n, w, G) \quad \dots(20)$$

$$A = f(\delta_{trim}, G) \quad \dots(21)$$

## 2.2 Effect of Flaps

Classical treatments of apparent longitudinal stick-free static stability have mostly ignored the effect of high lift devices such as flaps (and the application of power). Pilot experience has shown that the application of flaps during the approach and landing phase and application of power and retraction of flaps during the go-around may have a significant effect on trim and on the flow field surrounding the horizontal tail surface. The changes to flow field have a direct influence on the elevator forces required to trim the aeroplane during this configuration [14]. Figure 3, shows the net effect of the application of flaps on the span-wise lift distribution and wake vorticity experienced at the tail [12].

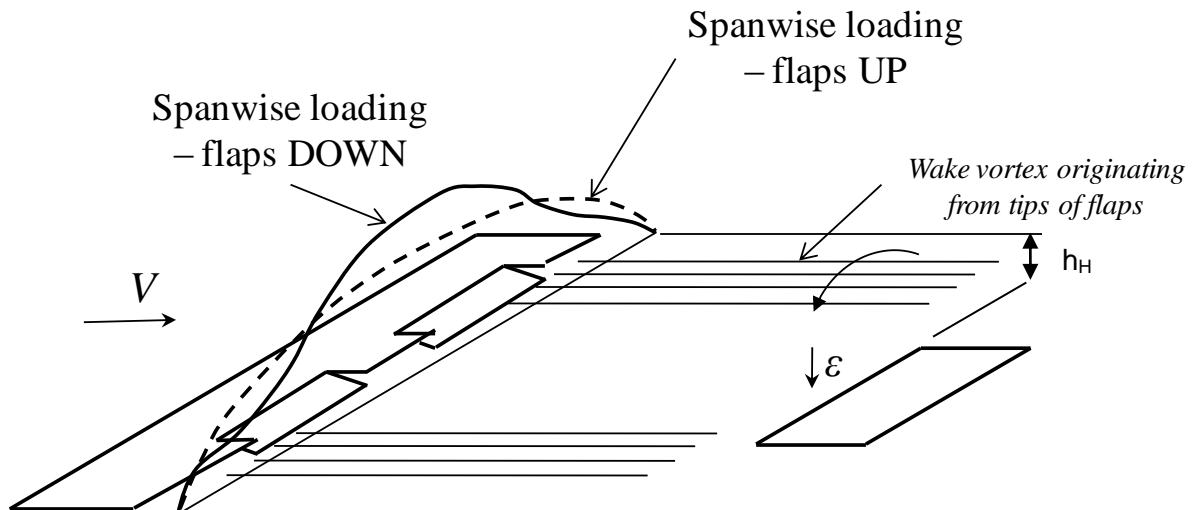


Figure 3, Effect of Part-span Flaps on Lift Distribution and Vorticity, adapted from [12]

The deflection of flaps tends to narrow the span of the trailing vortex, increasing the strength of the vortex behind the outer trailing edges of the flaps. There is a local increase in wing section camber resulting in a negative increment in  $C_{m_0}$  and a positive increment in  $C_{L_{wb}}$ , requiring the pilot to push the stick forward to command a downward deflection of the elevator to maintain a given trimmed airspeed condition. The corresponding increase in downwash at the tail, results in an increase to the downwash derivative ( $d\varepsilon/d\alpha$ ) and downwash constant ( $\varepsilon$ ).

## 2.3 'What-if' Analysis using MATLAB

In order to explore the effects of parameter variations on apparent stick-free longitudinal static stability, a script was written using MATLAB, a commonly used numerical computing environment and fourth generation computer programming language [15]. This enabled 'what-if' analysis due to contributory factors and the variation of stick forces and stick force gradients to be estimated using Equation...(15) and Equation ...(19). A flowchart defining the processing logic is shown in Figure 5. Using estimated design data for a Cessna 150M, a typical high-wing, 2 seat light aeroplane (Figure 4 and Appendix A, Table A-1), graphs of stick force and stick force gradients were developed with the following parameter variations:-

- Weight ( $W$ )
- CG ( $h$ )
- Elevator Gearing ( $G$ )
- Downwash derivative ( $d\varepsilon/d\alpha$ )



**Figure 4, A Typical High Wing Light Aeroplane - Cessna C150M (library photograph)**

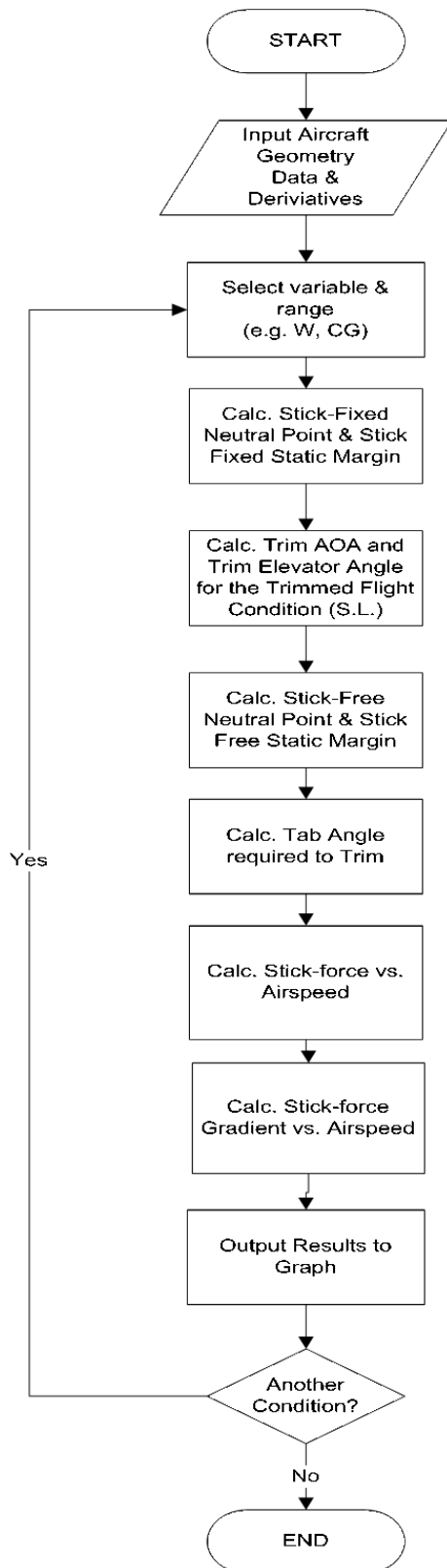


**Figure 5, Flowchart for Estimation of Apparent Longitudinal Stick-Free Static Stability**

For selected aeroplane geometry, configurations and trim conditions, the downwash at the tail ( $\varepsilon$ ) was determined using Perkins & Hage [18]. The corresponding downwash derivative ( $d\varepsilon/d\alpha$ ), was determined using the DATCOM empirical methods for subsonic downwash both with and without flap deflection [17].

The estimated results are presented Figures 6~10. The variation of stick force versus airspeed for one nominated parameter at a time, was estimated from a generic, high-wing light aeroplane for a given trim condition in the cruise, at  $V_E = 84$  kt and  $W = 1600$  lbf MTOW at sea level in standard atmosphere conditions.

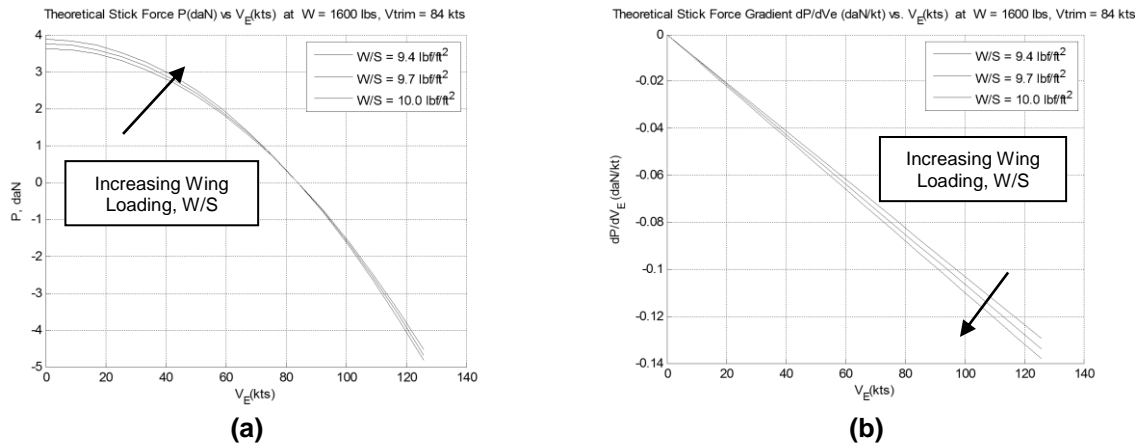


Figure 6, MATLAB Output: Variation of (a) Apparent Longitudinal Stick-free Static Stability and (b) Stick Force Gradient with Wing Loading,  $W/S$  (lbf/ft<sup>2</sup>)

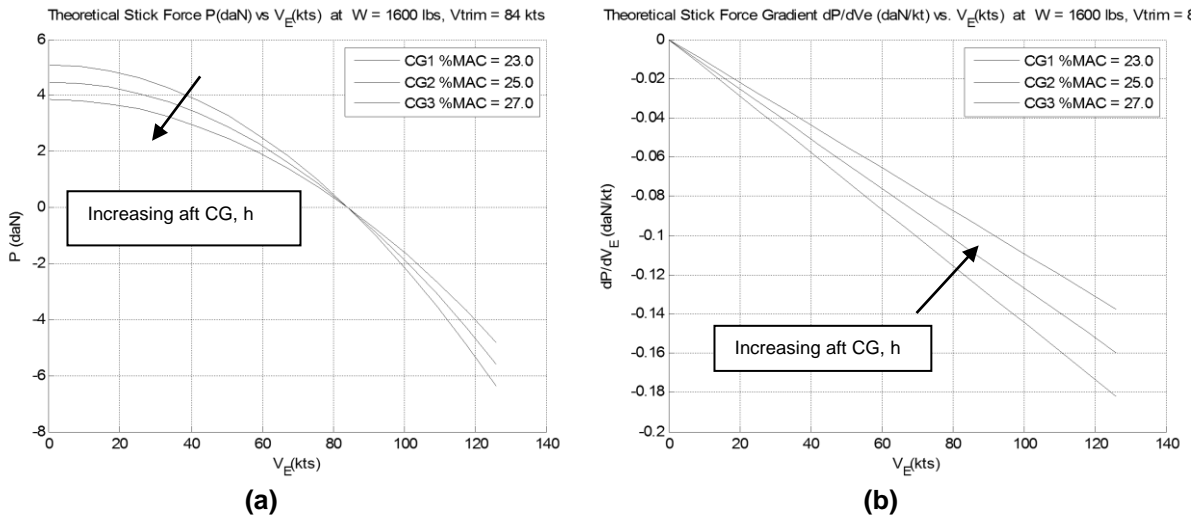
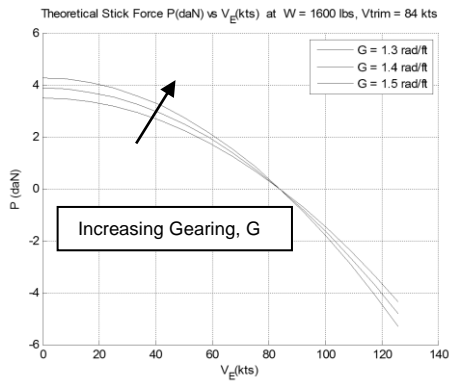
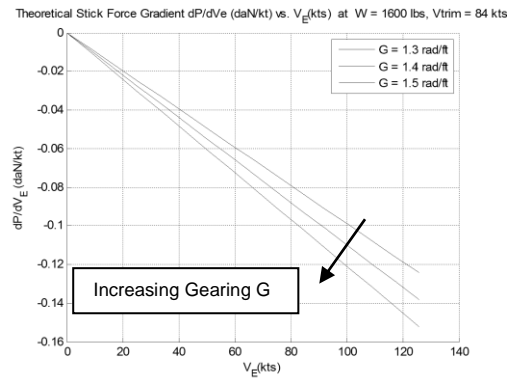


Figure 7, MATLAB Output: Variation of (a) Apparent Longitudinal Stick-free Static Stability and (b) Stick Force Gradient with  $h$  (CG %MAC)

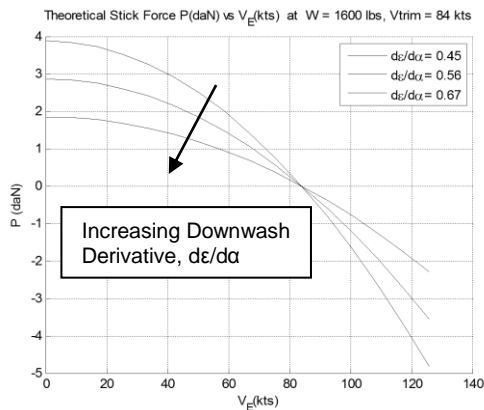


(a)

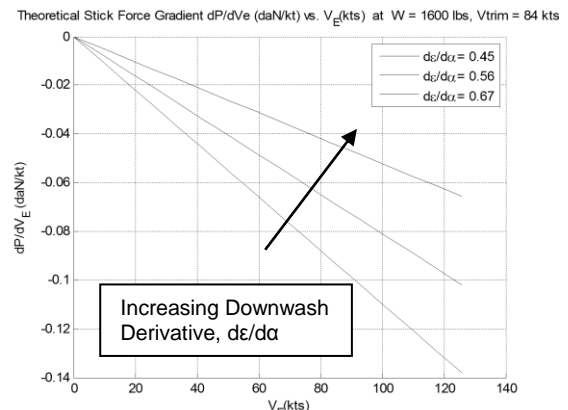


(b)

**Figure 8, MATLAB Output: Variation of (a) Apparent Longitudinal Stick-free Static Stability and (b) Stick Force Gradient with Elevator Gearing,  $G$  (rad/ft)**

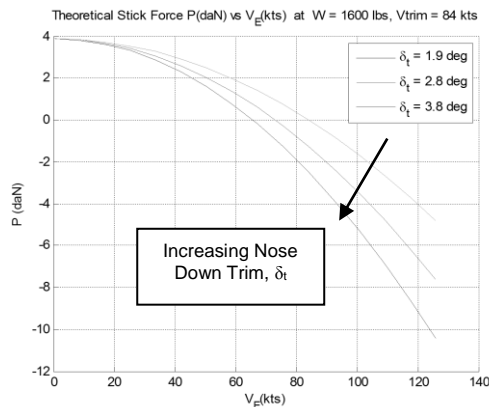


(a)

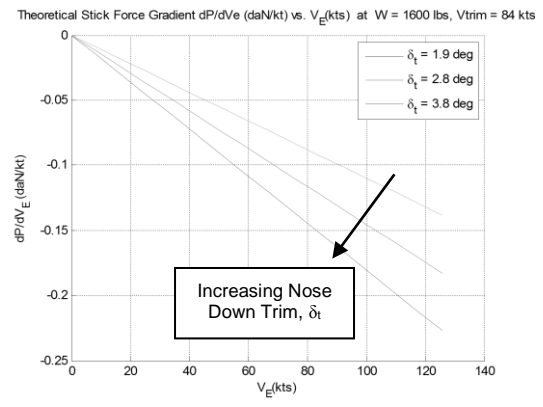


(b)

**Figure 9, MATLAB Output: Variation of (a) Apparent Longitudinal Stick-free Static Stability and (b) Stick Force Gradient with Downwash Derivative,  $dε/dα$**



(a)



(b)

**Figure 10, MATLAB Output: Variation of (a) Apparent Longitudinal Stick-free Static Stability and (b) Stick Force Gradient with Elevator Trim  $δ_t$  (deg)**

The theoretical results of this MATLAB 'what-if' analysis are shown in the above figures may be summarised as follows in Table 2:-

**Table 2, Summary of MATLAB Predicted Qualitative Effects of Parameter Changes on Stick Force Coefficients**

<b>Parameter</b>	<b>Variable during flight?</b>	<b>Change Effect on Y-intercept (coefficient 'C')</b>	<b>Change Effect on Gradient (coefficient 'A')</b>
Wing Loading, $w$ increasing	No (negligible, typically <10%)	Increase	Increase
Elevator Gearing, $G$ increasing	No	Increase	Increase
Elevator Trim Tab, $\delta_t$ increasing Nose Down	Yes, dependent upon configuration and phase of flight	None	Increase
CG, $h$ move AFT increasing arm	Yes, dependent upon fuel tank configuration & layout	Decrease	Decrease
Downwash Derivative $d\varepsilon/d\alpha$ , increasing	Yes, dependent on power and flap setting	Decrease	Decrease

It can be seen from the table that both Y-intercept (coefficient 'C') and gradient (coefficient 'A') are dependent upon by the forward movement of CG, increased elevator gearing and increased wing loading in line with known theory. The elevator trim tab has no effect on coefficient 'C'. The downwash factor has strong influence on the coefficient 'A' and 'C' but is less well documented and not explicitly highlighted. This is an area of specific interest during approach and climb-out phases of flight where flaps may be used. Each individual aeroplane, will have its own combination of characteristics. The following sections of the paper show the application of theory to particular aircraft examples using a combination of physical measurements and flight conditions.

## 2.4 Theoretical Estimation of Apparent Longitudinal Stick-free Static Stability for the Cessna 150M

Using initial trim conditions for the cruise, landing with 30 degrees of flap and climb with flaps up, at full power, the theoretical apparent stick-free longitudinal static stability was determined for the typical, popular two-seat training aircraft, Cessna Model C150M (Figure 4) using the MATLAB script. Note that US-built Cessnas are prefixed 'C' before the model number and French built Cessnas are prefixed 'F' i.e. C150M is a US-built Cessna 150 Model 'M', whereas F150M is the equivalent model built in France by Reims-Cessna. Design characteristics of the C150M are shown in Appendix A, Table A-1. The Cessna 150 and Cessna 152 model groups do not utilise downsprings or bobweights in the elevator control circuit to modify stick force gradient. Tailplane, elevator and trim tab hinge moments used were based upon published manufacturers' data for similar airframes [16]. The initial trim conditions correspond to actual trim conditions obtained during test flights conducted prior to the development of the MATLAB script. Adjustments were made for pressure altitude effects and conversion from indicated to equivalent airspeed ( $V_E$ ) for valid comparison with actual flight test data later. The results are presented in the following sections.

Using the developed theory and trim conditions as specified in Appendix A, Table A-2 theoretical results obtained for the cruise configuration are shown in Figure 11 (a) & (b). Estimations of the downwash at the tail and downwash derivative were prepared using Hoak [17] and Perkins & Hage [18]. The results show that for the cruise configuration the theoretical stick force gradient at a trim speed of 89 kt is approximately 0.086 daN/kt. The Y-intercept (coefficient 'C') is approximately 3.82 daN.

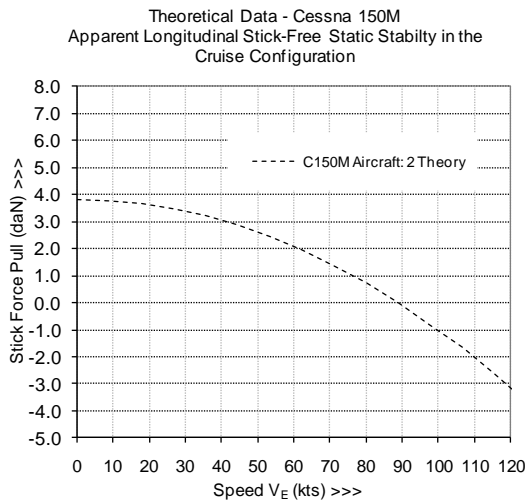
From the trim conditions specified in Appendix A, Table A-3, and the landing configuration with 30 degrees of flap, power for level flight at a trim speed of 67 knots, the theoretical stick force gradient reduces significantly (Figure 12 (a) & (b)) to only -0.018 daN/kt with Y-intercept (coefficient 'C') reducing to 0.60 daN.

In the climb with trim conditions as specified in Appendix A, Table A-4, Figure 13 (a) & (b) shows results with full power and zero degrees of flap, the stick force gradient at trim speed of 67 kt is approximately -0.110 daN/kt. The Y-intercept (coefficient 'C') remains the same as in the cruise configuration (3.82 daN), with the power setting used in the climb (56% BHP) being close to that used for cruising level flight at 89 kt (54% BHP).

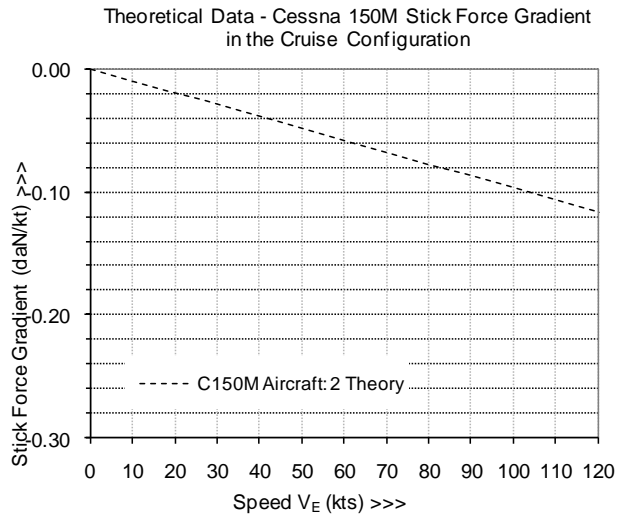
A summary of all theoretical results for the estimation of apparent longitudinal stick-free static stability for the Cessna 150M is shown in Table 3, below.

**Table 3, Theoretical Stick Force Gradients at  $V_{Trim}$  for the Cessna C150M for the Climb, Cruise and Landing Configurations**

Test No.	Description of Tests	$V_{trim}$ (kt)	Power (% BHP)	W (lbf)	CG (%MAC)	Stick Force Gradient (daN/kt)
1	Apparent LSS Climb Power	67	56	1580	27.00	-0.110
2	Apparent LSS Cruise Configuration	89	54	1580	27.00	-0.086
3	Apparent LSS Landing Configuration 30 Flap	68	54	1580	27.00	-0.018

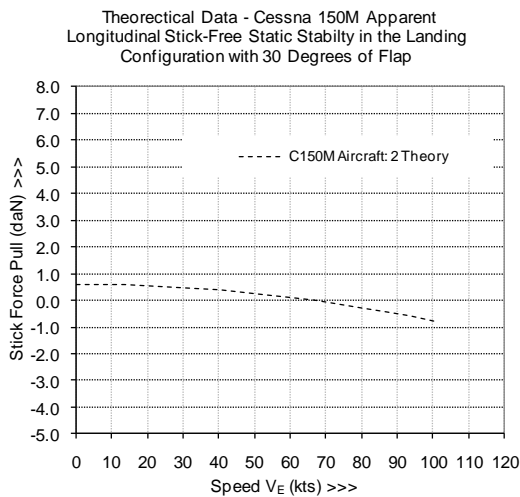


**(a)**

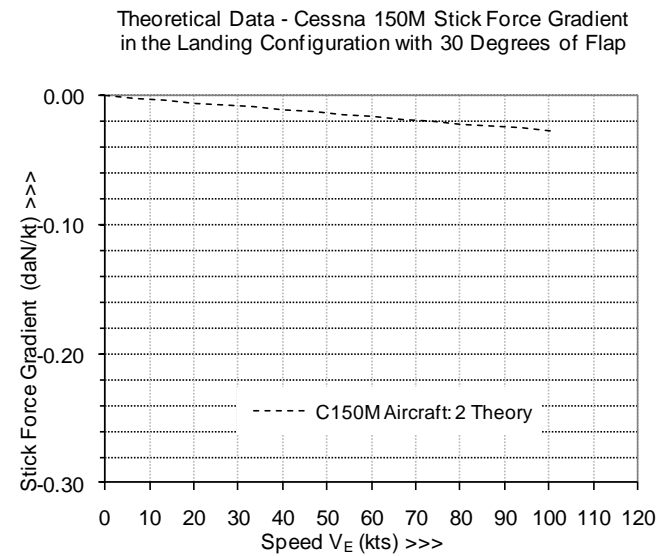


**(b)**

**Figure 11, Theoretical Estimation of Apparent Longitudinal Stick-free Static Stability for Cessna C150M in the Cruise**

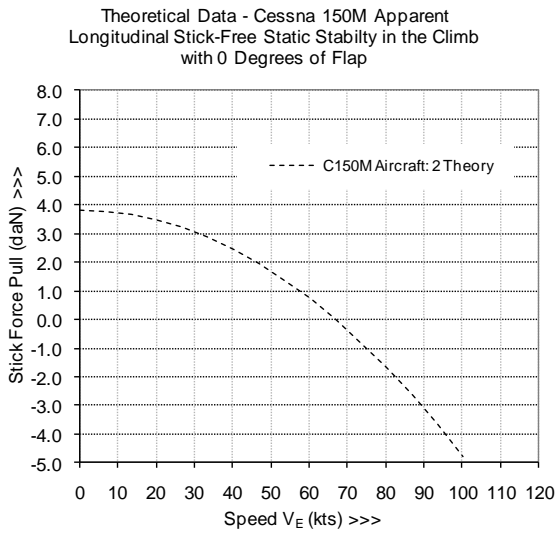


**(a)**

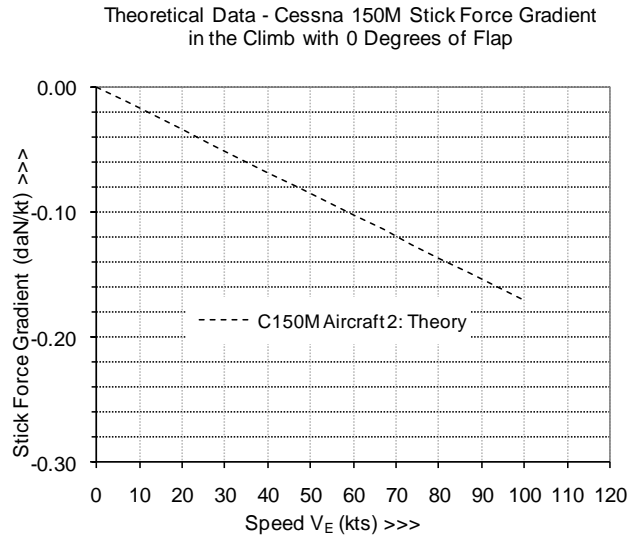


**(b)**

**Figure 12, Theoretical Estimation of Apparent Longitudinal Stick-free Static Stability for Cessna C150M in the Landing Configuration, with 30 degrees of Flap**



(a)



(b)

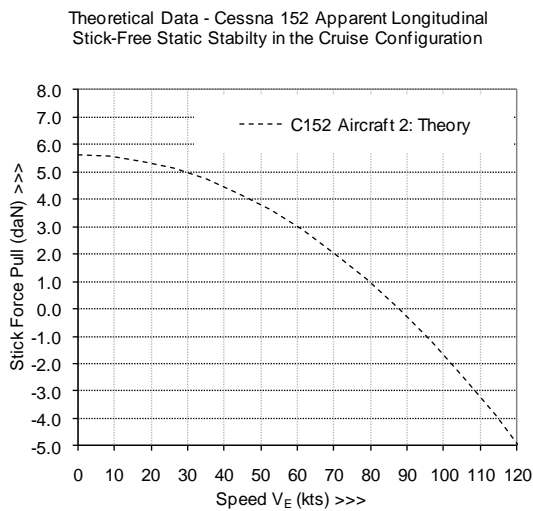
Figure 13, Theoretical Estimation of Apparent Longitudinal Stick-free Static Stability for Cessna C150M in the Climb with 0 degrees of Flap

## 2.5 Theoretical Estimation of Apparent Longitudinal Stick-free Static Stability for the Cessna 152

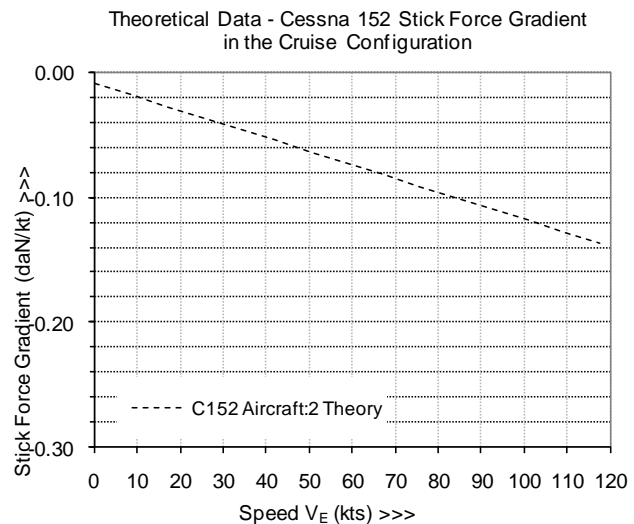
In addition to the Cessna 150M, theoretical estimates were also prepared for the Cessna C152 (1982 Model), with design characteristics as shown in Appendix A, TableA-1. Results for the Cessna C152 Model are presented in Figure 14, Figure 15 & Figure 16. In the cruise configuration at a trim speed of 88 kt, the theoretical stick force gradient is approximately -0.100 daN/kt with a Y-intercept value of 5.62 (coefficient 'C'). In the landing configuration with 30 degrees of flap and approach power, gradient at trim speed (67 kt) reduces to -0.058 daN/kt with a Y-intercept value (coefficient 'C') of 1.95 daN. For the climb configuration, the gradient at trim speed (67 kt) is closer to that of the cruise at -0.170 daN/kt with a Y-intercept the same as in the cruise, 5.62 daN. A summary of all theoretical results is presented in Table 4 below.

**Table 4, Theoretical Stick Force Gradients at  $V_{Trim}$  for the Cessna C152 in the Climb, Cruise and Landing Configurations**

Test No.	Description of Tests	$V_{trim}$ (kt)	Power (% BHP)	W (lbf)	CG (%MAC)	Stick Force Gradient at $V_{Trim}$ (daN/kt)
1	Apparent LSS Climb Power	67	66	1670	23.39	-0.170
2	Apparent LSS Cruise Configuration	88	53	1670	23.39	-0.100
3	Apparent LSS Landing Configuration 30 Flap	68	63	1670	23.39	-0.058

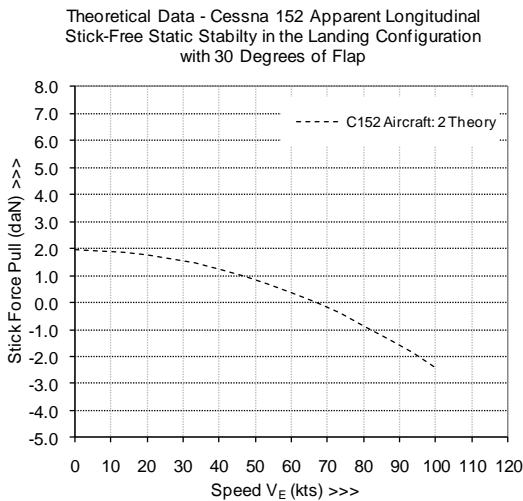


(a)

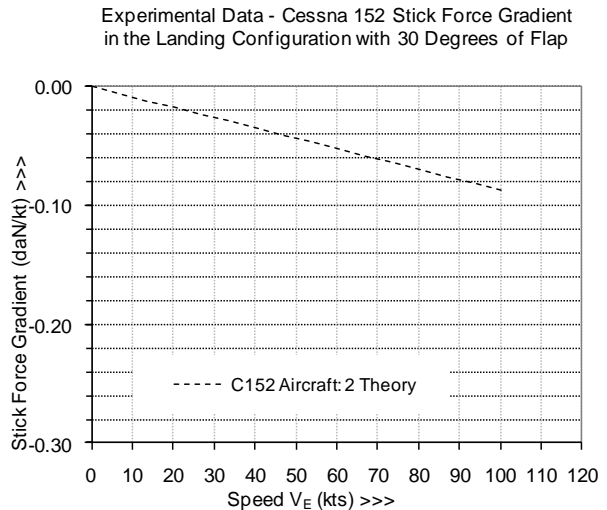


(b)

**Figure 14, Theoretical Estimation of Apparent Longitudinal Stick-free Static Stability for Cessna C152 in the Cruise**

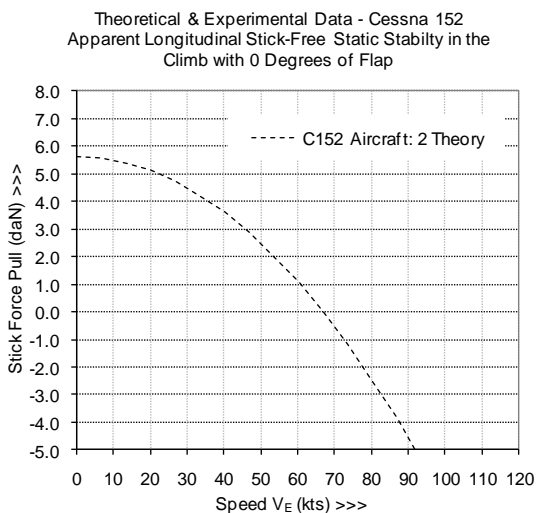


(a)

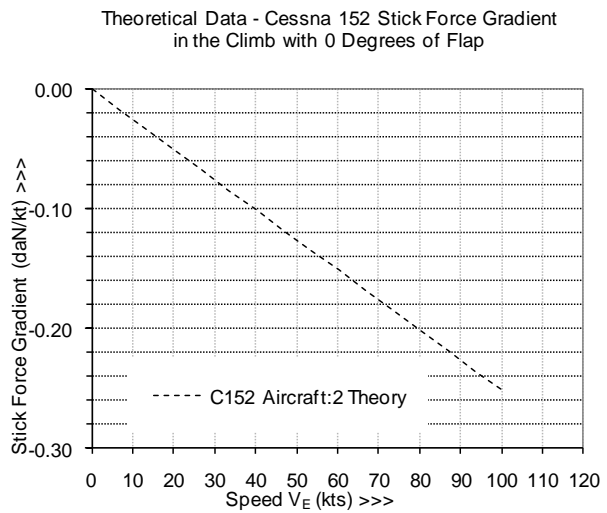


(b)

**Figure 15, Theoretical Estimation of Apparent Longitudinal Stick-free Static Stability for Cessna C152 in the Landing Configuration, with 30 degrees of Flap**



(a)



(b)

**Figure 16, Theoretical Estimation of Apparent Longitudinal Stick-free Static Stability for Cessna C152 in the Climb with 0 degrees of Flap**

## 2.6 Summary of Theoretical Results

Table 5 provides a final summary of theoretical stick force gradients for the Cessna C150M and C152 in the climb, cruise and landing configurations. The comparison of stick force gradients by configuration for both Cessna models shows that the cruise configurations result in the highest stick force gradients. The stick force gradient decreases in the climb configuration and decreases further still in the landing configuration with 30 degrees of flap. It should be noted that the effects of power have not been modelled in the theoretical analysis at this time. In the case of the Cessna 150M modelled with a noticeably further aft CG, the predicted stick force gradient is approaching zero and is approaching neutral stick-free static stability.

**Table 5, Summary of Theoretical Stick Force Gradients in the Climb, Cruise and Landing Configurations**

Test No.	Description of Tests	Stick Force Gradient at $V_{Trim}$ (daN/kt)	
		Cessna C150M	Cessna C152
1	Apparent LSS Climb Power	-0.110	-0.170
2	Apparent LSS Cruise Configuration	-0.086	-0.100
3	Apparent LSS Landing Configuration 30 Flap	-0.018	-0.058

### 3 FLIGHT TEST

#### 3.1 Introduction

To compare theoretical and experimental data for apparent stick-free longitudinal static stability, the Cessna C150 and C152 aeroplanes were selected since these were readily available and widely used in the UK training environment. Over 31,340 Cessna C150/C152s were built over a period of 26 years from 1959 to 1985 [19]. Key design features and pilots operating handbook performance are compared and are summarised in Appendix A, TableA-1.

The Cessna C150 was first built in 1959 and manufactured in 13 major variants model 'A' to 'M', including the introduction of an aerobatic model (Cessna Aerobat) from 1970 onwards (model 'K'). Production of the Reims-Cessna 150s (prefix 'F' not 'C') began in 1967. The Cessna C152 replaced the Cessna C150 in 1978 and this incorporated a larger engine to improve the climb-out, and cruise performance. In addition to the engine change came a different propeller, the net effect of these changes was a substantial (up to 1.5") forward movement of the CG together with a 70 lbf increase in MTOW. At the same time the 'barn door', fowler flaps were reduced to a maximum movement of 30 degrees, to further improve low speed handling and the climb-out performance during a go-around. The spin entry and recovery techniques for the Cessna C150M and C152 types were consequently different as noted in the 1981 technical addendum published by Cessna [20].

In phase 1 of the test programme (Table 6), examples of Cessna aeroplane models C150L, C150M and C152 were selected from a number of flying schools throughout the UK to gather experimental data at a range of CG positions (Phase 1). After an initial assessment of one example of each model, it was decided to repeat the same tests on at least two additional examples of the Cessna C150M and C152 to explore fleet-wide attributes (Phase 2 & 3). All aeroplanes used in the flight test programme were standard and un-modified.

**Table 6, Flight Test Programme**

Phase 1 – Aircraft 1			Phase 2 – Aircraft 2		Phase 2 – Aircraft 3		
	CG1	CG2	CG3	CG1	CG1		
C152	1637 lbf @23.81%	1491 lbf @25.28%		C152	1670 lbf @23.39%	F152	1655 lbf @23.78%
F150L	1599 lbf @25.28%						
F150M	1600 lbf @25.68%	1425 lbf @27.22%	1598 lbf @27.90%	C150M	1580 lbf @27.00%	F150M	1599 lbf @25.87%
Crew:	2	1	2	Crew:	2	Crew:	2

#### 3.2 Flight Test Equipment

Test equipment was selected for portability and to avoid changing the aeroplane certification state or interfere with safe aeroplane operation. All electronic devices were required to operate from their own internal power supply with no interference to standard cockpit instrumentation, radio/navigation aids or intercom.

Traditional handheld equipment such as ruler, stopwatch, spring balance force gauge and kneeboard mounted test cards were used. The location of flight tests was determined by aeroplane availability, with five different airfields used in total over a period of 13 months.

A portable GPS system with current database was used to locate position in unfamiliar airspace, freeing the pilot to concentrate upon the tests. A compact, portable and lightweight wide-angle lens video camera was used to capture cockpit video for subsequent de-brief. This provided a useable view of cockpit instruments and the pilot and flight test engineer’s actions within the cockpit. A self-contained Appareo GAU 1000A [21] flight data recorder was used for all sorties and this was used in conjunction with AS Flight analysis software for post-sortie briefings, and subsequent analysis. Data was exported from AS Flight Analysis and converted to Microsoft Excel or Google Earth files for further review. This useful and inexpensive facility provided adequate quality inertial and positional data at approximately 4 Hz when signals were filtered for noise. A cross-calibration exercise for the flight data recorder was conducted against the embedded flight test instrumentation on Cranfield University’s National Flying Laboratory Centre (NFLC) BAe Jetstream 31 aeroplane. The results showed acceptable correlation for quasi-static flight conditions. A digital voice recorder, connected to a tie-clip microphone in one of the crew’s headsets provided adequate cockpit voice recording capability, and this could then be readily synchronised with both data from the flight data recorder, and from the cockpit camera. Appareo’s AS Flight Evaluator Software Version 1.05 was used for post-flight analysis, this enabled real-time playback of the test flights together with time series plots of major parameters of interest (e.g. geo-potential height, latitude, longitude, groundspeed etc.).

**3.3 Flight Test Method**

An initial ‘shakedown’ flight test was conducted in a Cessna C152 for all equipment as well as refinement of the test programme and procedures required to be repeated on all models. Flight tests for longitudinal static stability were conducted as part of a broader research programme [22]. Tests relevant to apparent longitudinal stick free static stability are shown in Table 7 below:-

**Table 7, Initial Scope of Flight Tests**

<b>Test No.</b>	<b>Description of Tests</b>	<b>Power</b>	<b>Flap (deg)</b>
1	Apparent LSS Climb Power	Full	0
2	Apparent LSS Cruise Configuration	Power for Level Flight	0
3	Apparent LSS Landing Configuration 30 Flap	Power for Level Flight	30

Although the principal area of interest for the flight tests was low-speed handling and stall characteristics, it was necessary to consider the aeroplane performance and handling as well since this might influence low speed handling. The test plan covered the apparent stick-free longitudinal static stability (LSS), all dynamic modes, climb and cruise performance, and stalling at the range of conditions permitted by the aeroplanes’ operating manuals. All testing was to be carried out within those conditions, and without going outside the conditions of each aeroplane’s Certificate of Airworthiness (CofA).

Before starting the test programme, the nominated Test Pilot had accumulated 57 hours on Cessna C150/C152 type with the Flight Test Engineer (also a qualified pilot) having 90 hours on C150/C152. Twelve test sorties were flown with 3 checkouts for the test pilot, using 8 aircraft totalling 25 hours and 35 minutes flying time over a 13-month programme.

All flights employed the same test pilot, using a calibrated handheld force gauge indicating in both kg and lbf and readable to an precision of 0.11 daN ( $\frac{1}{4}$  lbf) which was assumed to be the reading accuracy; airspeeds were recorded using the standard cockpit instrument then corrected to CAS and EAS using the Position Error Correction (PEC) charts in the respective operators manuals and tables. Aircraft weight and balance were determined from new load sheets based upon the last available new weighing of each aeroplane, actual fuel states from dipping aircraft fuel tanks and any changes in modification state since previous weighing. Supporting aircraft CofAs were checked for currency and all aircraft were therefore to be within the required control surface calibration tolerance limits.

### 3.4 Flight Test Results

Flight test experimental results for the apparent longitudinal stick-free static stability are presented in this section of the paper. All results have been adjusted for the effects of breakout force and friction, with the former being measured directly during the flight tests and the latter estimated by inspection of experimental data. Measured breakout and friction forces were generally low, ranging from 0.22~0.44 daN in pull (nose-up) and 0.11~1.11 daN in push (nose down). Figure 17 and Figure 18 are examples of experimental data before and after the removal of breakout and friction forces for a Cessna C152 (aircraft 2) and Cessna 150M (aircraft 2), respectively, in the cruise configuration. Using the adjusted data points, a 2<sup>nd</sup> order polynomial in  $V_E$  of the form  $P = C + AV_E^2$  as per Equation...(15) was applied using regression analysis and the MATLAB curve fitting tool ('cftool'), thus allowing subsequent comparison with predicted theory. The calculated polynomial coefficients ('A' and 'C') were then used to determine associated stick force gradients ( $dP/dV$ ) for all recorded airspeeds.

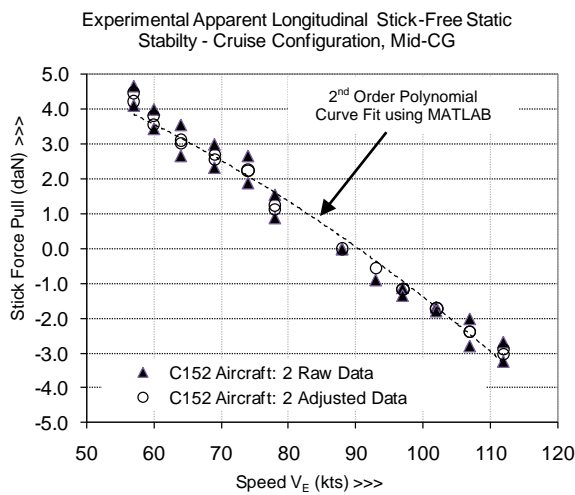


**Figure 17, Example: Experimental Apparent Longitudinal Stick-Free Static Stability C152 before and after removal of Breakout and Friction**

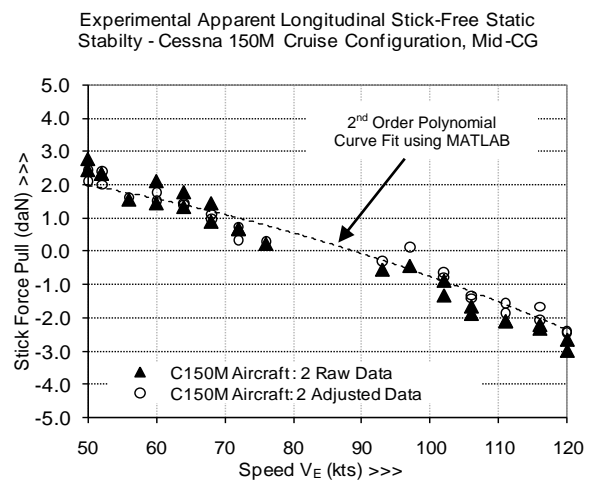


**Figure 18, Example: Experimental Apparent Longitudinal Stick-Free Static Stability C150M before and after removal of Breakout and Friction**

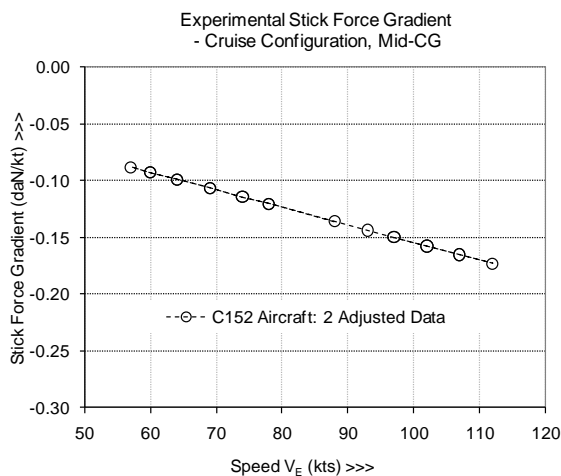


**Figure 19, Experimental Stick Force Gradient C152 determined using MATLAB Curve Fit Tool**

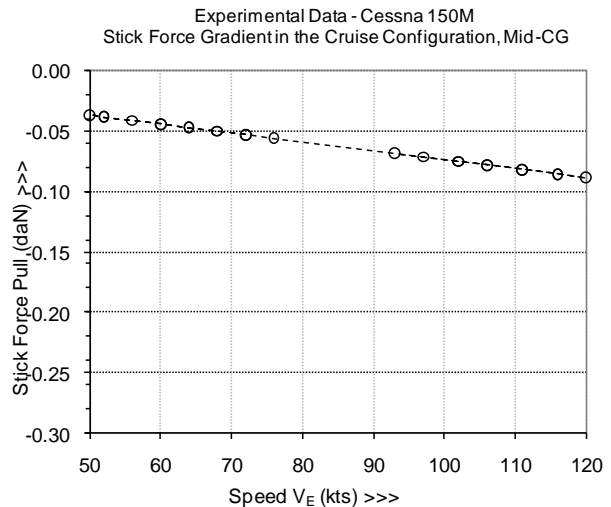


**Figure 20, Experimental Stick Force Gradient C150M determined using MATLAB Curve Fit Tool**

### 3.4.1 Apparent Longitudinal Stick-Free Static Stability of the Cessna 152

The flight test results for apparent longitudinal stick-free static stability in the cruise configuration for three Cessna 152 airframes (2 x C152 and 1 x F152) are shown in Figure 21 (a) & (b). These results and all subsequent results have been adjusted for the effects of breakout force and friction, with the former being measured during the flight tests and the latter estimated by inspection of the experimental data. Applying curve fit, the results show similarity in stick force gradients but also variation within the fleet. The variation can be partially attributed to the slightly different trim speeds used for the flight test and also the variation in TOW and CG. Stick force gradients at  $V_{Trim}$  for all three airframes are shown in Table 8.

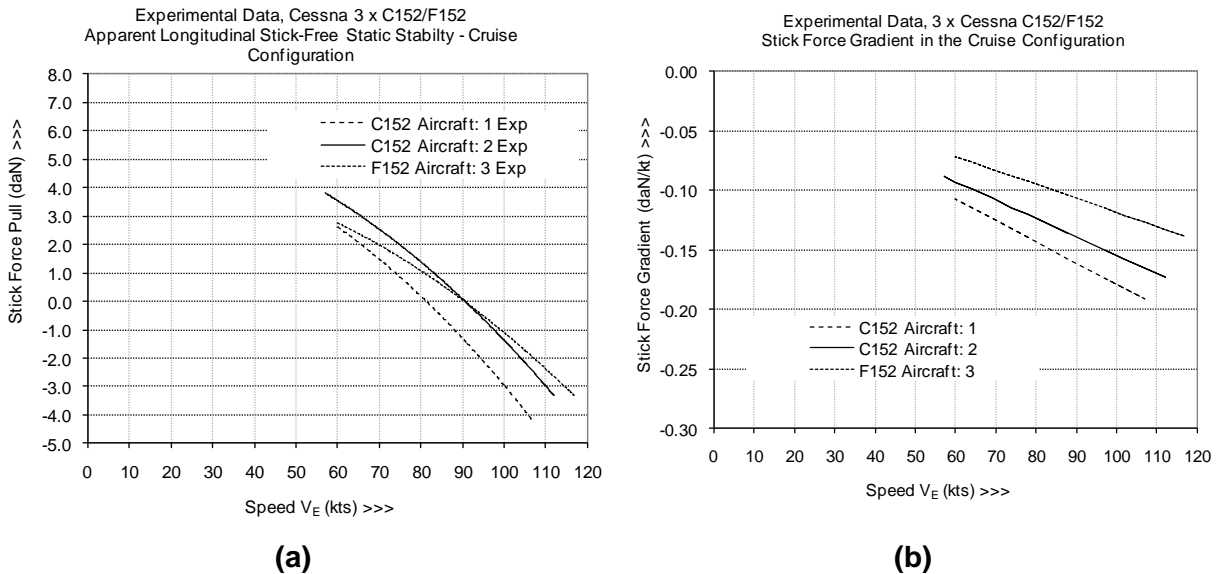


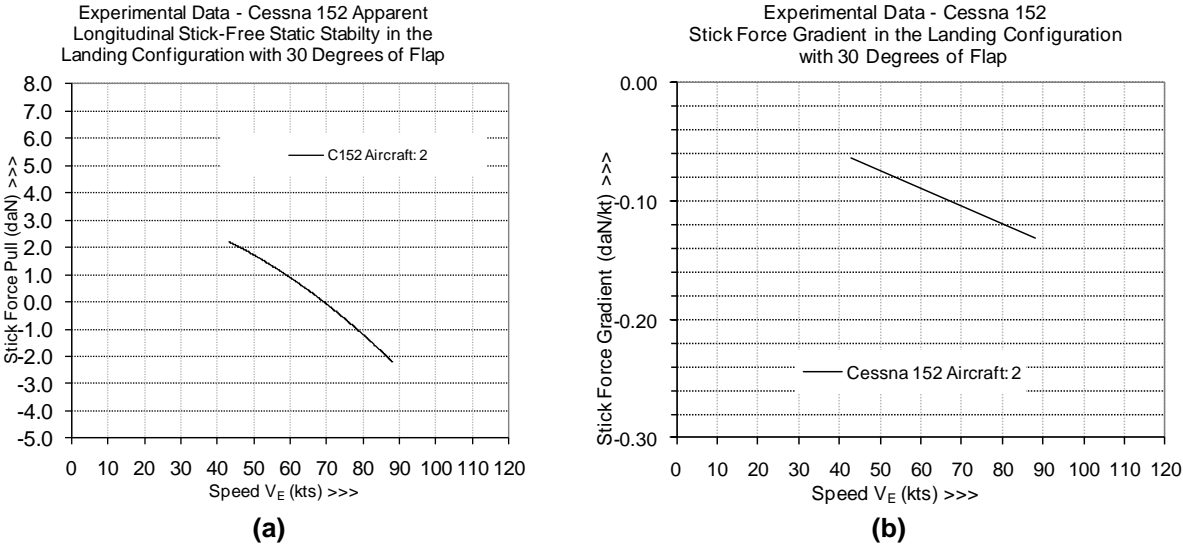
Figure 21, Apparent Stick-Free Longitudinal Static Stability (a) and Stick Force Gradient (b) for three Cessna C152/F152 Models in the Cruise Configuration

Table 8, Stick Force Gradients about the trim condition for 3 x Cessna 152/F152 Airframes in the Cruise at  $V_{Trim}$  from Figure 21 (b)

Description of Tests	Stick Force Gradient (daN/kt) at $V_{Trim}$		
	Aircraft 1: Cessna C152	Aircraft 2: Cessna C152	Aircraft 3: Cessna F152
Apparent LSS Cruise Configuration	-0.160	-0.140	-0.100

The results show a variation of stick force gradient at the trimmed airspeed from 0.10 to 0.16 daN/kt. Stick force gradient gives an indication of pilot perceptibility of stick force changes, a key requirement for aircraft certification as discussed earlier. All subsequent analyses of results are limited to one example airframe for clarity.

Experimental results for one representative Cessna C152 aeroplane (aircraft no.2) in the landing configuration are given in Figure 22, with the associated trim conditions noted in Appendix A, Table A-3. The results show a shallower stick force gradient than in the cruise configuration, with a gradient value of approximately -0.10 daN/kt at the trimmed approach airspeed of 66 kt. Power for level flight was used in this configuration (2,300 rpm), representing approximately 63% BHP.



**Figure 22, Apparent Stick-Free Longitudinal Static Stability (a) and Stick Force Gradient (b) for the Cessna 152 in the Landing Configuration with 30 Degrees of Flap**

Experimental results for the climb are given in Figure 23 with the associated trim conditions noted in Appendix A, TableA-4. The results show a stick force gradient higher than in the cruise configuration, with a gradient value of approximately -0.17 daN/kt at the trimmed best climb speed of 66 kt. Power for level flight was used in this configuration (2,300 rpm), representing approximately 66%BHP.

Fleet-wide differences were also present in both the landing and climb configurations for the Cessna 152 and Cessna 150M.

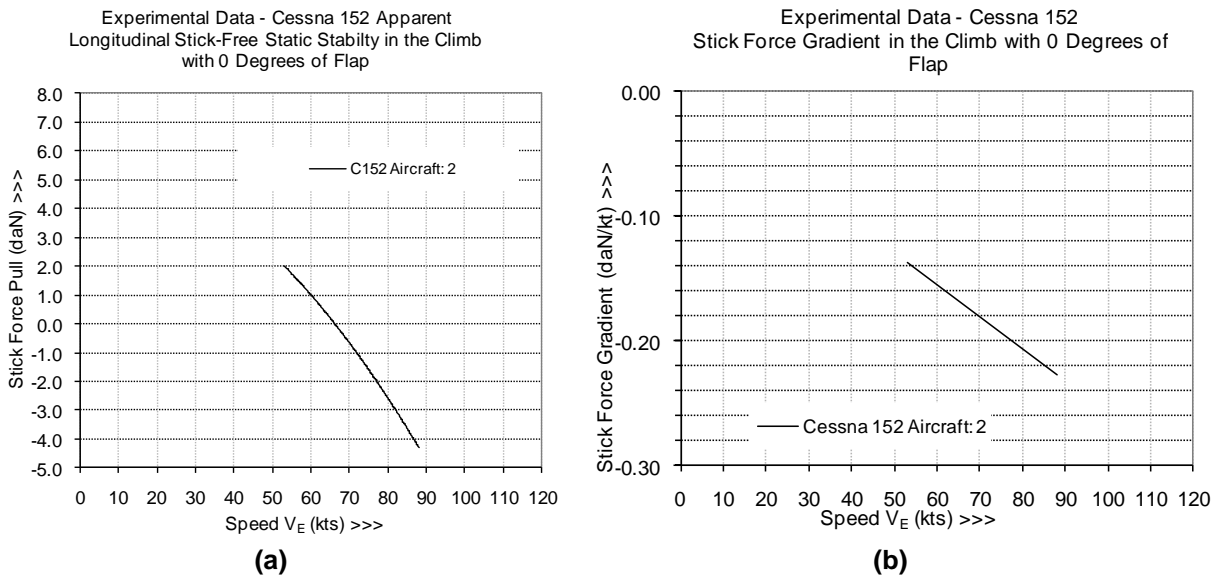
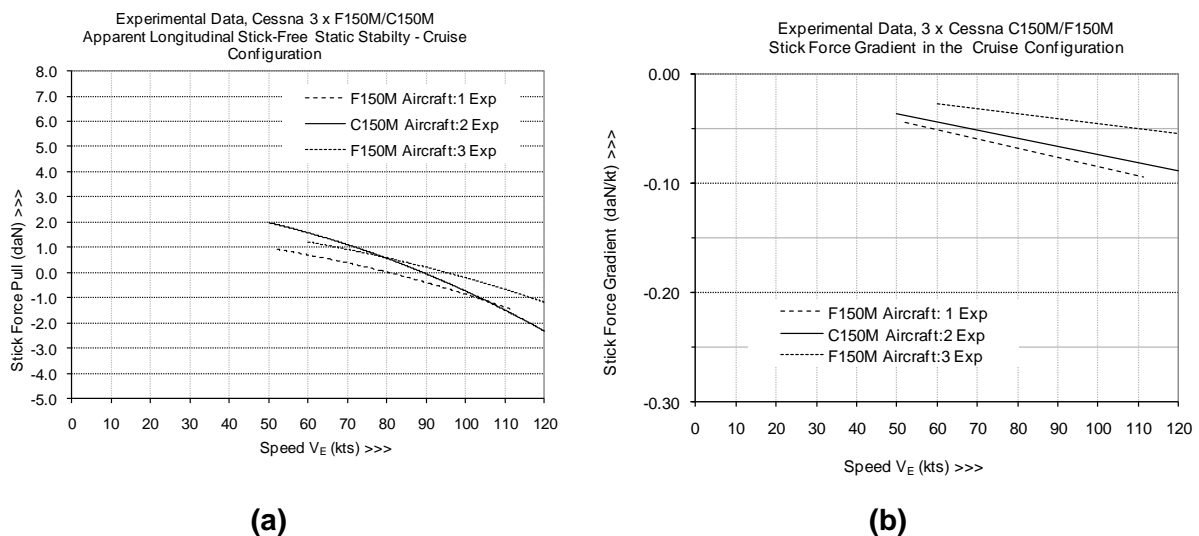


**Figure 23, Apparent Stick-Free Longitudinal Static Stability (a) and Stick Force Gradient (b) for the Cessna 152 in the Climb with 0 Degrees of Flap**

### 3.4.2 Apparent Longitudinal Stick-Free Static Stability of the Cessna 150M

Experimental flight tests were repeated for the Cessna C150M for further evaluation of the method. The results for the cruise, landing and climb configuration are presented in Figure 25, Figure 26 and Figure 27, with corresponding trim conditions shown in Appendix A, Table A-2, Table A-3 and Table A-4.

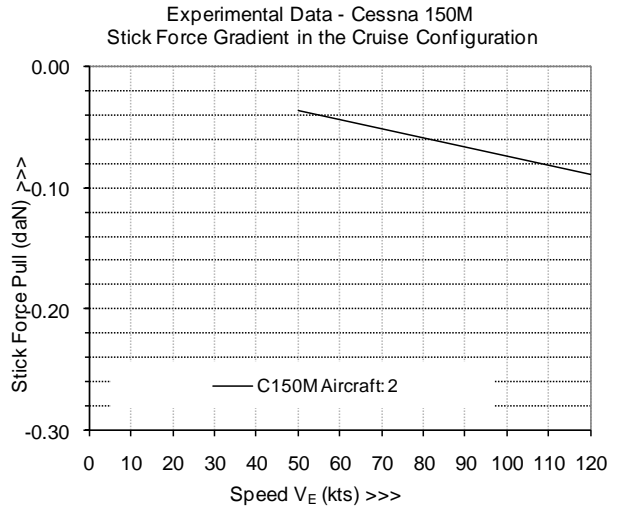
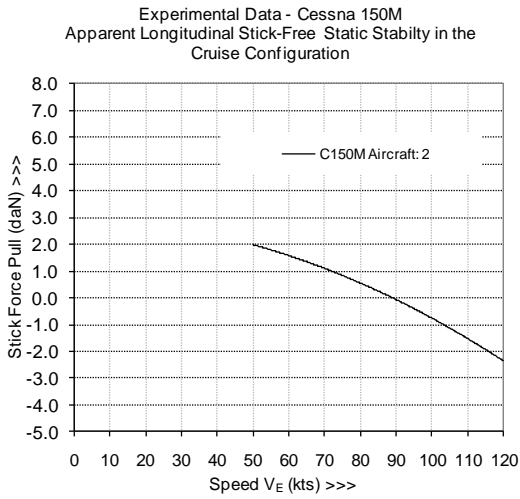
The flight test results for apparent stick-free longitudinal static stability in the cruise configuration for three Cessna C150M airframes (2 x F150M and 1 x C150M) are shown in Figure 24 (a) & (b). Applying curve fit, the results show similarity in stick force gradients but also indicate variation within the fleet. The variation can be partially attributed to the slightly different trim speeds used for the flight test and also the variation in TOW and CG. Stick force gradients at  $V_{Trim}$  for all three airframes are shown in Table 9.



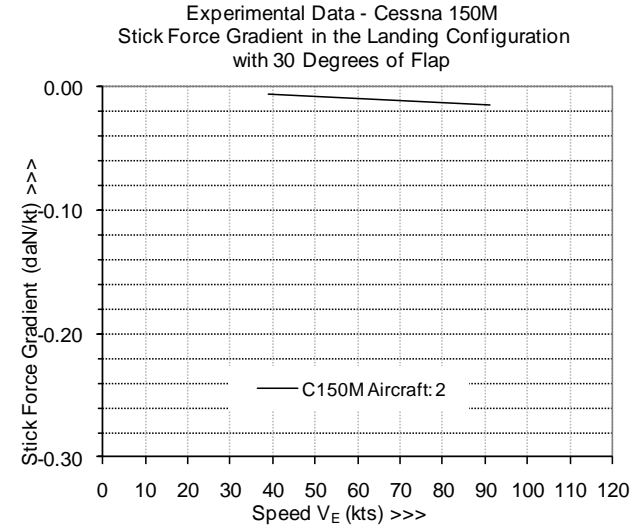
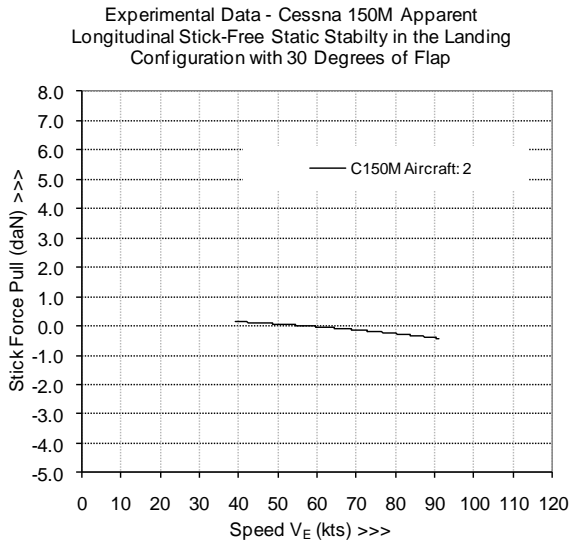
**(a)** **(b)**  
**Figure 24, Apparent Stick-Free Longitudinal Static Stability (a) and Stick Force Gradient (b) for three Cessna F150M/C150M Models in the Cruise Configuration**

**Table 9, The Comparison of Stick Force Gradients for 3 x Cessna F150M/C150M Airframes in the Cruise at  $V_{Trim}$**

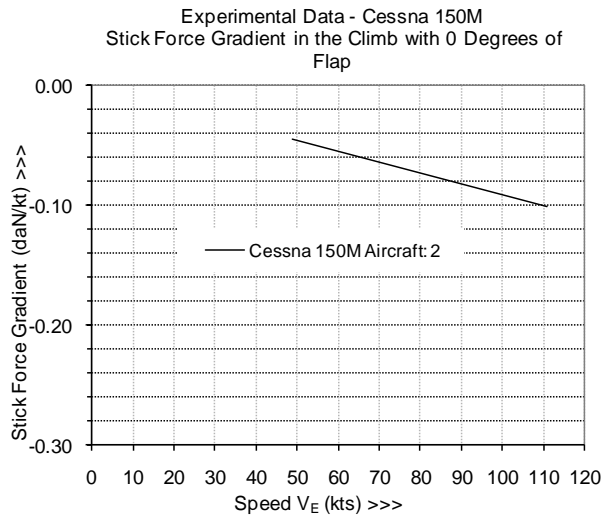
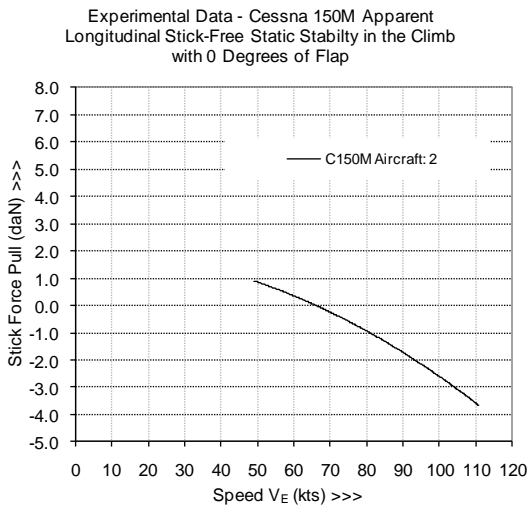
Description of Tests	Stick Force Gradient (daN/kt) at $V_{Trim}$		
	Aircraft 1:	Aircraft 2:	Aircraft 3:
	Cessna F150M	Cessna C150M	Cessna F150M
Apparent LSS Cruise Configuration	-0.070	-0.065	-0.040



(a) (b)  
**Figure 25, Apparent Stick-Free Longitudinal Static Stability (a) and Stick Force Gradient (b) for the Cessna 150M in the Cruise Configuration**



(a) (b)  
**Figure 26, Apparent Stick-Free Longitudinal Static Stability (a) & Stick Force Gradient (b) for the Cessna 150M in the Landing Configuration with 30 Degrees of Flap**



(a) (b)  
**Figure 27, Apparent Stick-Free Longitudinal Static Stability (a) & Stick Force Gradient (b) for the Cessna 150M in the Climb with 0 Degrees of Flap**

The results show stick force gradients at trim speeds of -0.060, -0.066 and -0.020 daN/kt for the climb, cruise and approach respectively. There is a significant reduction in stick force gradient as flaps are deployed. In all configurations, power for level flight was applied and therefore can be regarded as constant. A slight decrease in stick force gradient during the climb was observed.

### 3.4.3 Summary

The flight test results for stick force gradient at the trimmed airspeed are shown in Table 10 & Table 11. The airframes compared and presented are generally representative of the fleet. The stick force gradient at trim speed for the C150M airframe was highest in the cruise and lowest in the landing configuration. For the C152 airframe the gradient was highest in the climb and lowest in the landing configuration. Both airframes showed a significant decrease in stick force gradient in the landing configuration in particular. It should be note that for the C150M airframes tested, only the 30 degree flap position was selected. Application of a further 10 degrees of flap resulted in an even lower stick force gradient and in some cases, neutral or slightly negative stability was observed. The application of power and further forward CG appears to have had a direct and positive affect on stick force gradient in the climb and landing configuration for the C152.

**Table 10, Summary of Apparent Longitudinal Static Stability Flight Tests, Cessna C150M**

<b>Cessna C150M</b>		<b>CG:</b>	<b>27.00</b>	<b>@</b>	<b>1580 lbf</b>		
<b>Test No.</b>	<b>Description of Tests</b>	<b>(%MAC)</b>	<b>Power</b>	<b>% BHP</b>	<b>Flaps (deg)</b>	<b>Stick Force Gradient at <math>V_{Trim}</math> (daN/kt)</b>	<b>Breakout Force (Pull/Push daN)</b>
1	Apparent LSS Climb Power		Full	56	0	-0.060	0.44/-1.11
2	Apparent LSS Cruise Configuration		Level Flight	54	0	-0.066	0.33/-0.56
3	Apparent LSS Landing Configuration 30 Flap		Level Flight	54	30	-0.020	0.33/-0.22

**Table 11, Summary of Apparent Longitudinal Static Stability Flight Tests, Cessna C152**

<b>Cessna C152</b>		<b>CG:</b>	<b>23.39</b>	<b>@</b>	<b>1670 lbf</b>		
<b>Test No.</b>	<b>Description of Tests</b>	<b>(%MAC)</b>	<b>Power</b>	<b>% BHP</b>	<b>Flaps (deg)</b>	<b>Stick Force Gradient at <math>V_{Trim}</math> (daN/kt)</b>	<b>Breakout Force (Pull/Push daN)</b>
1	Apparent LSS Climb Power		Full	66	0	-0.170	0.44/-0.44
2	Apparent LSS Cruise Configuration		Level Flight	53	0	-0.136	0.44/-0.33
3	Apparent LSS Landing Configuration 30 Flap		Level Flight	63	30	-0.098	0.22/-0.11

## 4 COMPARISON OF THEORETICAL AND EXPERIMENTAL FLIGHT TEST RESULTS

In this section of the paper, theoretical and experimental data for apparent longitudinal stick-free static stability and stick force gradient are compared for two aeroplanes, the Cessna C150M (1975 model) and the Cessna C152 (1982 model) in the cruise, landing and climb configurations using the initial trim conditions established during the experimental flight tests. Adjustments were made for pressure altitude effects and all airspeeds were converted to equivalent airspeed (EAS) using aircraft pressure error correction charts. The cruise, landing and climb at full power are compared in the following sections.

### 4.1 Comparison of Theoretical and Experimental Results for the Cessna C150M

Using the same initial trim conditions as previously specified (see Appendix A, Table A-2, Table A-3 & Table A-4), a comparison of theoretical and experimental data for apparent longitudinal static stability and associated stick force gradient in the cruise for the Cessna C150M, aircraft 2 is given in Figure 28 (a) and (b). The results show reasonable correlation, with the stick force gradient at trim speed of 89 kt differing by only 0.020 daN/kt. Flaps were set to zero degrees with a cruise power setting enabling level flight.

In the landing configuration with 30 degrees of flap and power setting for level flight (Figure 29), the correlation is very good with a negligible stick force gradient difference of only +0.002 daN/kt. The stick force gradient is almost negligible in this configuration indicating near neutral stability.

Finally, in the climb configuration with zero flap and full power set (Figure 30), the correlation is also good, with a difference in stick force gradient of 0.050 daN/kt. It should be noted that for this particular airframe, full throttle was required to maintain level flight for all three configurations/trim speeds tested.

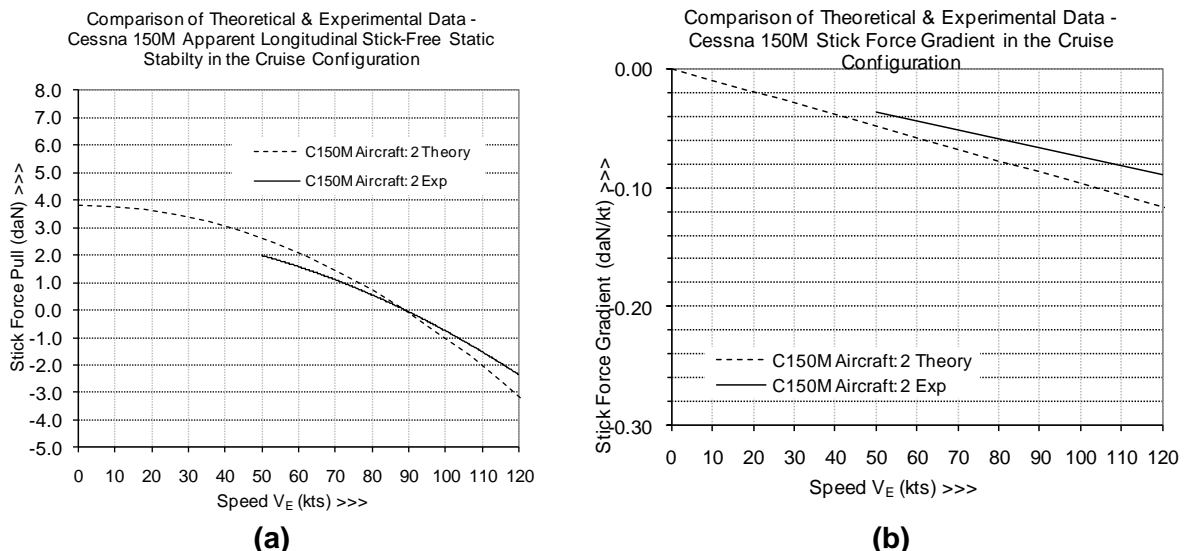
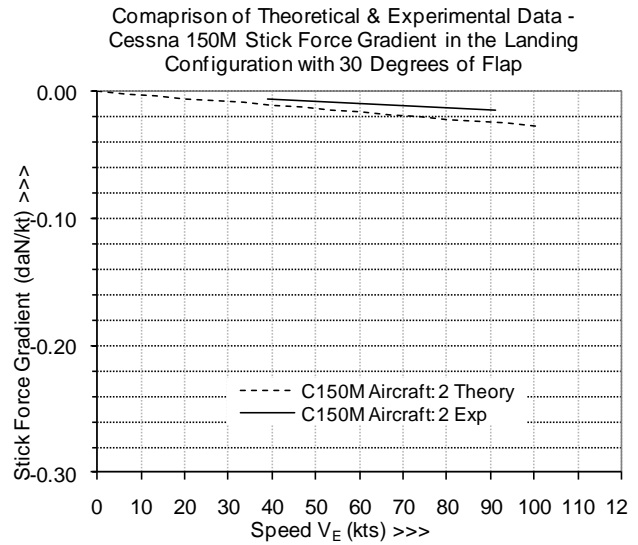
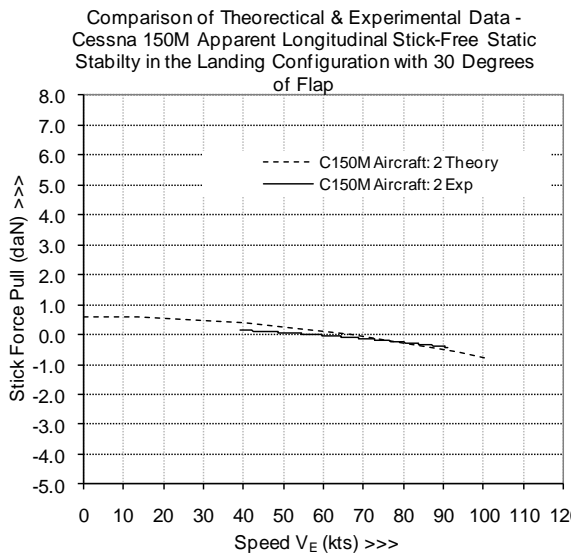


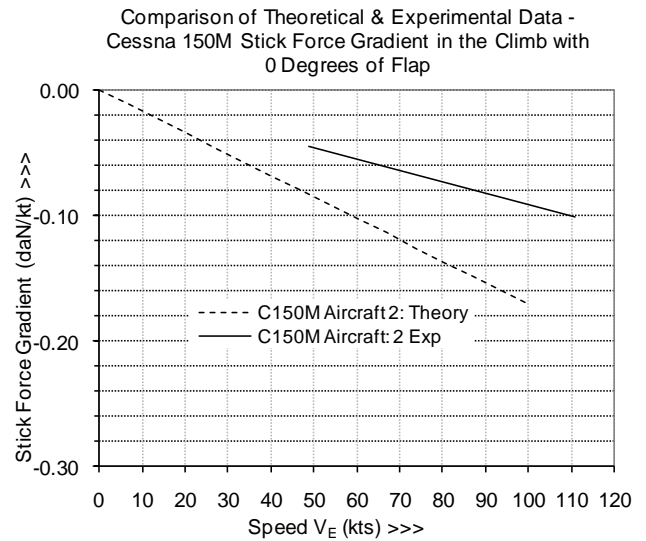
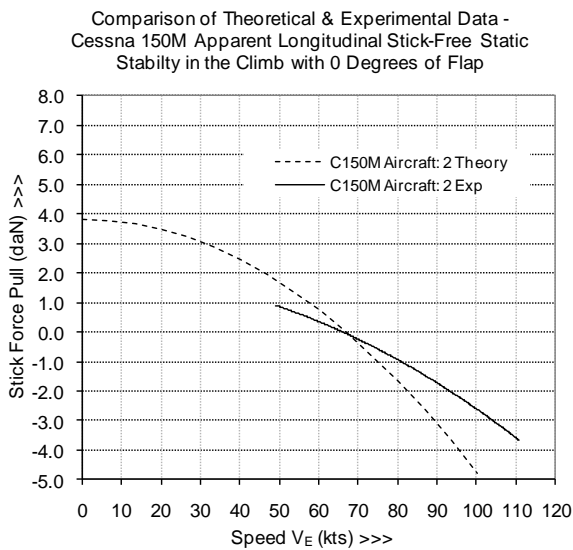
**Figure 28, Comparison of Theoretical and Experimental Data, Apparent Longitudinal Stick-free Static Stability - C150M in the Cruise Configuration**



(a)

(b)

**Figure 29, Comparison of Theoretical and Experimental Data, Apparent Longitudinal Stick-free Static Stability – Cessna C150M in the Landing Configuration with 30 Degrees of Flap**

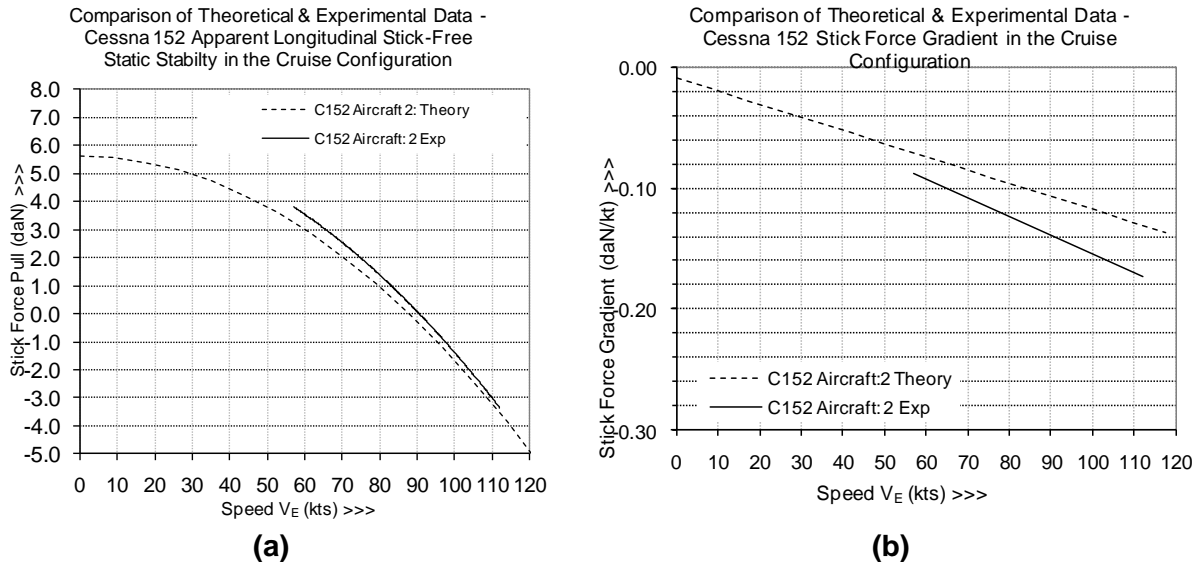


(a)

(b)

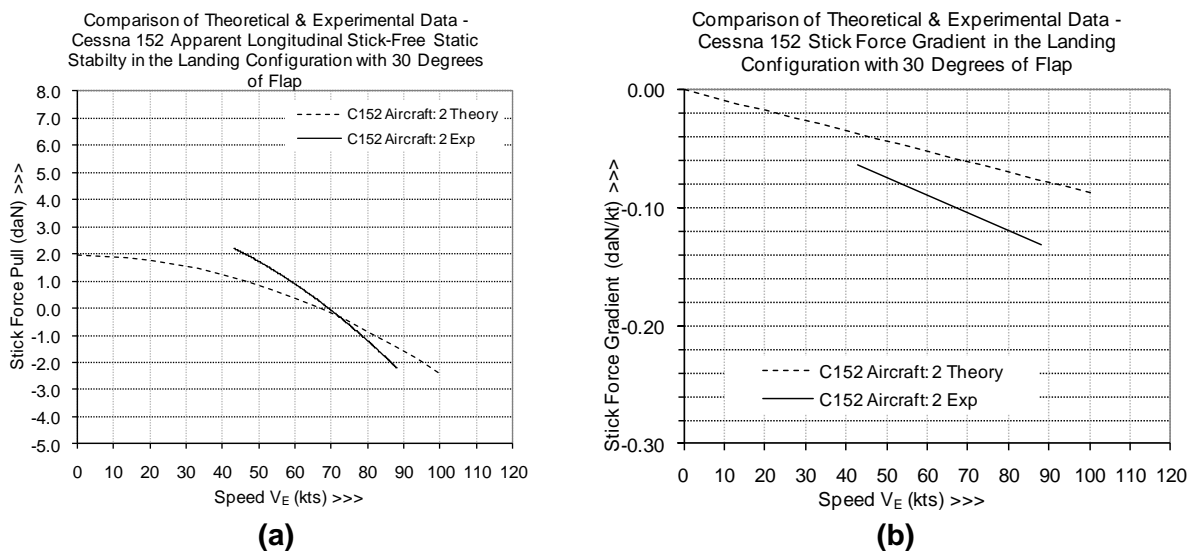
**Figure 30, Comparison of Theoretical and Experimental Data, Apparent Longitudinal Stick-free Static Stability – Cessna C150M in the Climb**

## 4.2 Comparison of Theory and Experimental Results for the Cessna C152



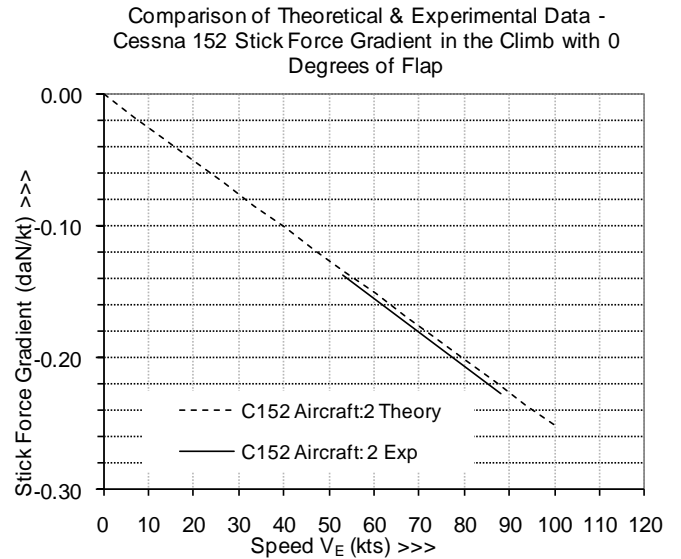
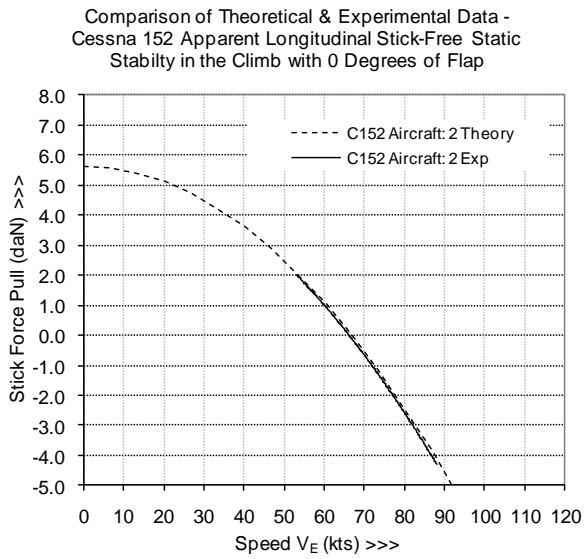
**Figure 31, Comparison of Theoretical and Experimental Data, Apparent Longitudinal Stick-free Static Stability - C152 in the Cruise Configuration**

Figure 31 show a comparison of theoretical and experimental data for the Cessna C152 in the cruise configuration with zero flap and power for level, cruising flight. The results show reasonable correlation with a stick force gradient difference of 0.045 daN/kt at the trim speed of 88 kt.



**Figure 32, Comparison of Theoretical and Experimental Data, Apparent Longitudinal Stick-free Static Stability – Cessna C152 in the Landing Configuration with 30 Degrees of Flap**

Similarly, in the landing configuration (Figure 32) with 30 degrees of flap set and power for level flight, the difference in stick force gradient at the trim condition is -0.040 daN/kt, indicating poor correlation. It should be noted that the power setting required to maintain level flight at the initial trim speed of 67 kt for this airframe was 10% greater than the cruise configuration.



**(a)** **(b)**  
**Figure 33, Comparison of Theoretical and Experimental Data, Apparent Longitudinal Stick-free Static Stability – Cessna C152 in the Climb**

Finally, in the climb with zero flap and full power (66% BHP) the difference between stick force gradients at the trim speed of 67 kt was zero, showing excellent correlation (Figure 33).

### 4.3 Summary of Results Comparison

A summary of the comparative results for stick force gradients at the trim condition are given in Table 12 and Table 13. It can be seen that overall, all results for stick force gradients are accurate to within 0.00 to 0.05 daN/kt. It should be noted that allowances for power effects were not made in the theoretical analysis. As experimental stick force gradients decrease the differences between theoretical and experimental values increase. Breakout forces and friction have a greater influence when stick forces are low and tend to increase the gradient locally about the trim condition. Notwithstanding this limitation, Figure 17 & Figure 18 as presented earlier, show that the curve fit is a reasonable approximation both with and without adjustment for breakout and friction when the measured breakout and friction forces were less than 0.44 daN.

**Table 12, Comparison of Theoretical and Experimental Stick Force Gradients at  $V_{Trim}$  for the Cessna C150M in the Climb, Cruise and Landing Configurations**

Test No.	Description of Tests	$V_{Trim}$ (kt)	% BHP	THEORY (daN/kt)	EXP. (daN/kt)	DIFFERENCE= THEORY-EXP. (daN/kt)
1	Apparent LSS Climb Power	67	56	-0.110	-0.060	-0.050
2	Apparent LSS Cruise Configuration	89	54	-0.086	-0.066	-0.020
3	Apparent LSS Landing Configuration 30 Flap	68	54	-0.018	-0.020	0.002

**Table 13, Comparison of Theoretical and Experimental Stick Force Gradients at  $V_{Trim}$  for the Cessna C152 in the Climb, Cruise and Landing Configurations**

Test No.	Description of Tests	$V_{Trim}$ (kt)	% BHP	THEORY (daN/kt)	EXP. (daN/kt)	DIFFERENCE= THEORY-EXP. (daN/kt)
1	Apparent LSS Climb Power	66	66	-0.170	-0.170	0.000
2	Apparent LSS Cruise Configuration	88	53	-0.100	-0.136	0.036
3	Apparent LSS Landing Configuration 30 Flap	66	63	-0.058	-0.098	0.040

## 5 DISCUSSION AND CONCLUSIONS

The application of classical theory for the estimation of apparent stick-free longitudinal static stability has been traditionally applied to the cruising phase of flight only. However, extension of the theory (by consideration of the effects of tail downwash/flap changes) subsequently validated by experimentation, has enabled assessment of the climb-out, approach and landing phases of flight to be completed. Stick force gradient accuracy within 0.05 daN/kt has been proven for a high-wing, low-tail aeroplane model by comparison with flight test data. The accuracy of the modelling increases with stick force gradient and the method gives a reasonable indication of the trending effect of selected parameters and hence aircraft 'feel'. The analysis has shown that for the high-wing, low-tail aeroplanes tested, there is a trend towards a possible stick force gradient 'reversal' when flaps are deployed to maximum settings. The net effect of this is that stability becomes neutral. Analysis has shown that when the horizontal tail arm between tail and wing is short and the vertical distance is small, the rate of change of downwash angle with alpha changes significantly, hence there is reduced tail damping. The rapid change in stick force gradient considerably alters the 'feel' of the aircraft, especially during the approach and landing phase. Care should be taken in the initial design stage of a new aeroplane to avoid significant trim changes as this can give rise to decreased stability and increased pilot workload. In the cruise and climb configuration, the effects of CG and wing loading dominate the stick force gradient but in the landing configuration, combination of both aft CG and increased downwash at the tail due to flaps, considerably changes the stick forces and gradients, modifying sensory cues to the pilot.

In comparing theoretical and experimental data, key assumptions have been re-examined and the following points are likely to have contributed to the observed differences. For the experimental data, it is possible that errors were present due to the following:-

- calibration errors between flap position and indication (in the Cessna 150M);
- differences in elevator control surface movements and gearing;
- excessive wear/usage in control system linkages;
- aero-elastic effects including 'blow-back' of the flap angle due to increased local dynamic pressure;
- excess friction and breakout forces (up to 0.44 daN);
- limited precision of the handheld force gauge (within 0.11 daN) and hysteresis;
- inaccurate weight and balance records;
- different propellers fitted to the same aircraft models (fine versus coarse pitch);

Within the range of airframes tested during the experimental flight testing, fleet-wide differences were apparent for the same aircraft model and year of manufacture and these may be due to:-

- type/model of propeller fitted and differences in flight performance and propeller effects on tail downwash;
- the number, type and quality of paint coatings applied;
- weight and balance differences due to damage repairs to the aeroplane, fitting of different equipment, general ageing, accumulation of dirt/foreign objects and moisture;
- aerodynamic effects of removal of wheel fairings and dents to wing leading edge;

For the theoretical data, the accuracy is limited by underlying assumptions in the modelling, namely:-

- estimations of hinge moments in sub-sonic flight are dependent upon numerous factors including Reynolds number, control surface deflection, nose shape, horn geometry, chord ratio, gap, tab geometry, angle of attack, overhang and trailing edge angle [23];
- in the examples used herein, the hinge moment estimations appear reasonable and are based upon established manufacturers' data for similar aeroplane models;
- however, estimations are reported to be generally accurate to within 30% [23], probably due to their lack of boundary layer modelling [18];
- estimations of the downwash due to flaps are on the limits of published theory [17];
- both the direct and in-direct effects of power affect stability and downwash derivative and have been excluded;
- non-linearities in control system linkages are present.

Notwithstanding the accuracy as noted, there is value in the application of classical theory for the estimation of apparent longitudinal stick free static stability. However, due consideration is necessary for downwash effects due to flap deflection and power settings and in addition stick force gradients must be regarded as having potential to tend towards becoming neutral or negative resulting in undesirable handling qualities. The method could prove useful, for example in determining the likely acceptability of a proposed design, or as part of the safety assessment for flight testing of a new prototype.

## **6 FURTHER WORK**

Further validation of the method should include aeroplanes of different wing/tail combinations i.e. low-wing/mid-tail, low-wing/T-tail etc. In addition, friction, mass, aero-elastic and power effects should be considered to further improve the accuracy of the estimation methods. Both direct and indirect power effects on stability should be considered, direct effects due to the position of the engine thrust line relative to the vertical CG and indirect effects due to propeller wash over the wings, flaps and horizontal tailplane in all configurations. For flight test stick force measurements, digital load cells should be used for improved accuracy and increased data points in all airspeed regions. This will also accelerate the reduction of data and data analysis. The use of non-viscous CFD to estimate the downwash and downwash derivatives rather than data sheet approach would also improve accuracy and reduce analysis time.

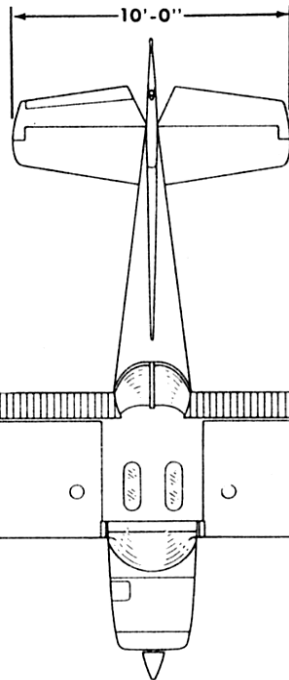
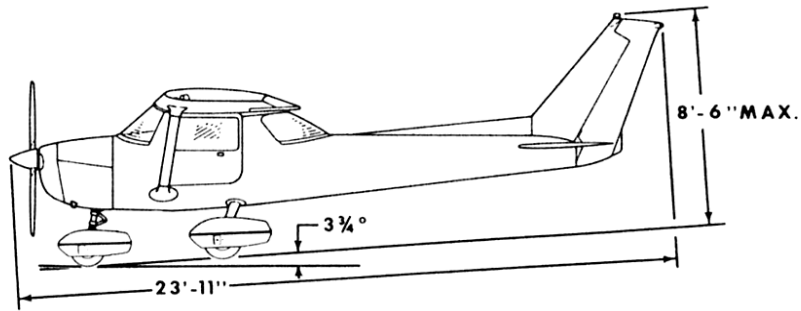
## **ACKNOWLEDGMENTS**

Thanks to Dr. Mark Young and Dr. Cristinel Mares at Brunel University for their support through this research. We also gratefully acknowledge the financial support of the Thomas Gerald Gray Charitable Trust Research Scholarship Scheme. We are also indebted to Roger Bailey, Chief Test Pilot of the National Flying Laboratory at Cranfield University, for providing assistance in the calibration of the flight test equipment using Cranfield's Jetstream J31 flying classroom.

**APPENDIX A**

**Table A-1, Characteristics of Cessna C150M and C152**

	<b>C150M (1975)</b>	<b>C152 (1982)</b>
<b>Powerplant</b>	Continental, generating 100 BHP at 2,750 rpm	Lycoming, generating 110 BHP at 2,550 rpm
<b>Propeller</b>	McAuley Standard	McAuley Gull Wing
<b>MTOW</b>	1600 lbf	1670 lbf
<b>CG Range</b>	31.5-37.5" (19.9-30.1%MAC)	31.0-36.5" (19.1 – 28.4 %MAC)
<b>Flap Range</b>	0-40°	0-30°
<b>Flap mechanisation</b>	2 way switch, variable spring/latch characteristics. No detents.  Indicator in left hand door pillar.	4 position gated switch, detents at 0/10/20/30°. Indicator adjacent to switch
<b>V<sub>so</sub> @MTOW, Aft CG (CAS)</b>	42 knots	41 knots
<b>V<sub>so</sub> @MTOW, Aft CG (IAS)</b>	31 knots	41 knots



**NOTES:**

1. Wing span shown with strobe lights installed.
2. Maximum height shown with nose gear depressed, all tires and nose strut properly inflated, and flashing beacon installed.
3. Wheel base length is 58".
4. Propeller ground clearance is 12".
5. Wing area is 160 square feet.
6. Minimum turning radius (\* pivot point to outboard wing tip) is 24' 8".

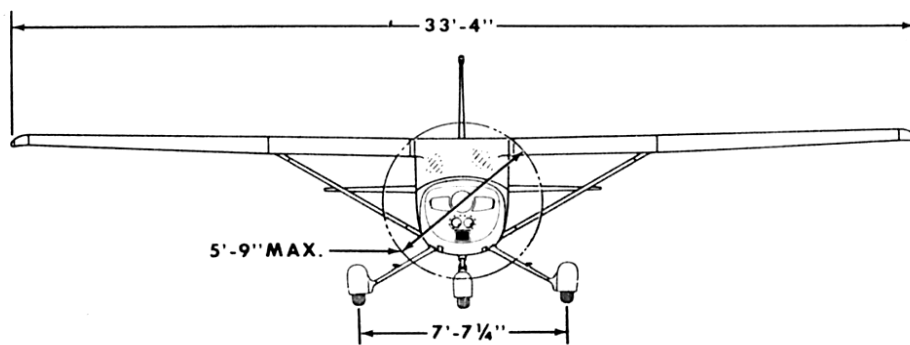
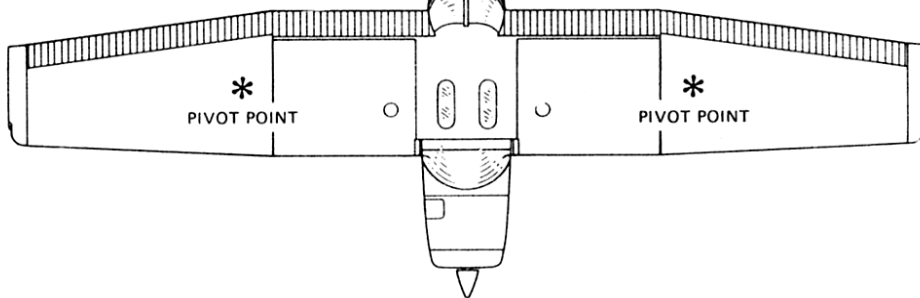


**Figure A-1, Cessna C150M (1975) Three View Diagram [24]**

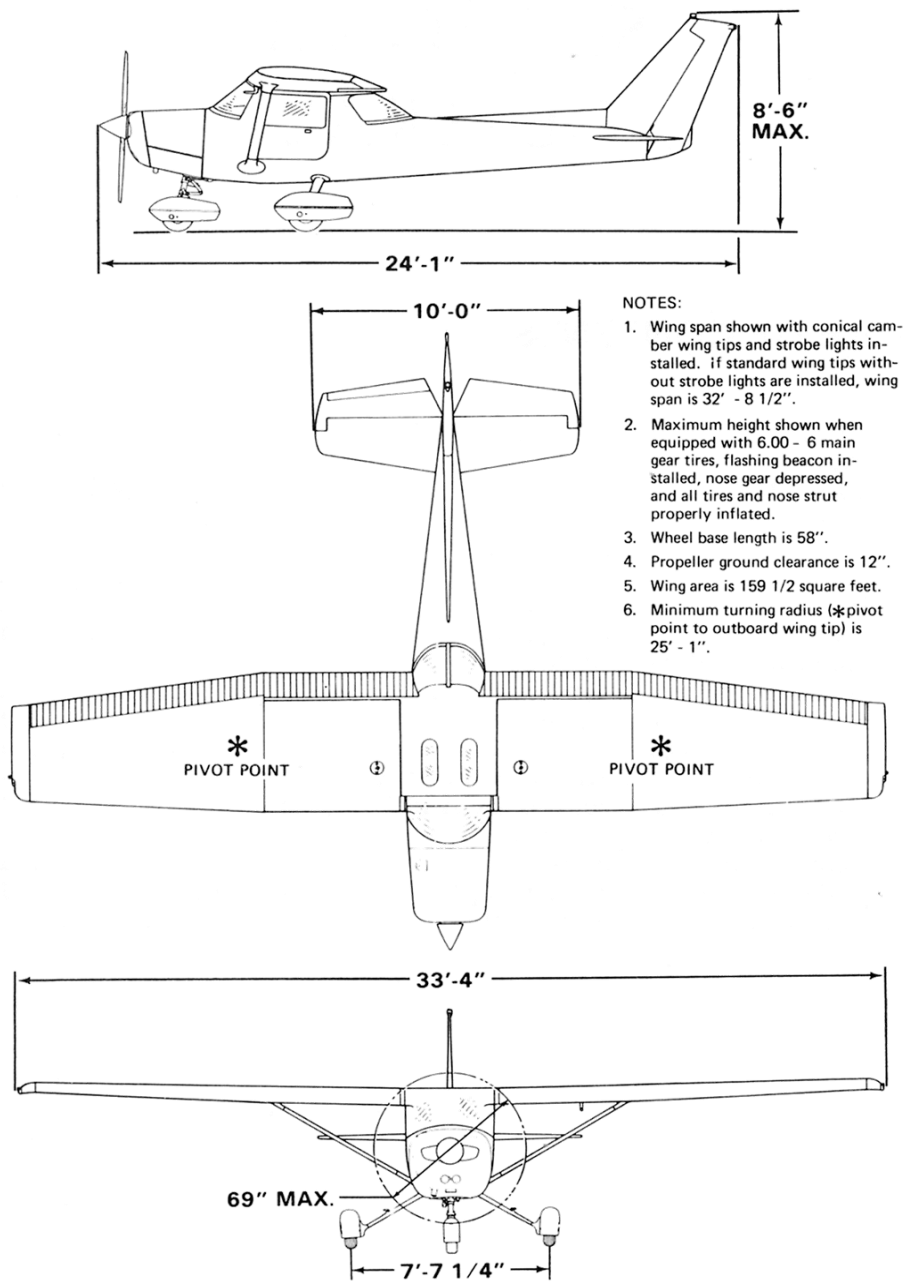


Figure A-2, Cessna C152 (1982) Three View Diagram [25]

**Table A-2, Initial Parameters for Comparison of Theoretical and Experimental data in the Cruise Configuration**

Parameter	Cessna C150M (1975) ‘Trainer’	Cessna C152 (1982)
Weight, $W$ (lbf)	1580	1670
Airspeed $V_E$ (kt)	89	88
Mean Height - sHp (ft)	3,600	3,500
Flaps, $\delta_f$ (deg)	0	0
Elevator Trim, $\delta_{t_{trim}}$ (deg)	8	8
Power (% BHP.)	54	53
Wing Loading $w$ (lbf/ft <sup>2</sup> )	9.91	10.47
CG aft of datum (inches)	35.69	33.56
CG as a percentage of CG range (%)	69.8	46.6
CG, 2 POB @ TOW, $h$ (%MAC)	27.00	23.39
Estimated Elevator Gearing, $G$ (rad/ft)	1.39	1.50
Estimated downwash at tail, $\varepsilon$ (deg)	2.190	2.088
Estimated Downwash Derivative, $\frac{d\varepsilon}{d\alpha}$	0.4464	0.4464

**Table A-3, Initial Parameters for Comparison of Theoretical and Experimental data in the Landing Configuration with 30 Degrees of Flap**

Parameter	Cessna C150M (1975) ‘Trainer’	Cessna C152 (1982)
Weight, $W$ (lbf)	1580	1670
Airspeed $V_E$ (kt)	67	68
Mean Height - sHp (ft)	0	3,500
Flaps, $\delta_f$ (deg)	30	30
Elevator Trim, $\delta_{t_{trim}}$ (deg)	-3	-1
Power (% BHP.)	54	63
Wing Loading $w$ (lbf/ft <sup>2</sup> )	9.91	10.47
CG aft of datum (inches)	35.69	33.56
CG as a percentage of CG range (%)	69.8	46.6
CG, 2 POB @ TOW, $h$ (%MAC)	27.00	23.39%
Estimated Elevator Gearing, $G$ (rad/ft)	1.39	1.50
Estimated downwash at tail, $\varepsilon$ (deg)	7.960	7.860
Estimated Downwash Derivative, $\frac{d\varepsilon}{d\alpha}$	0.8000	0.8000

**Table A-4, Initial Parameters for Comparison of Theoretical and Experimental data in the Climb**

Parameter	Cessna C150M (1975) 'Trainer'	Cessna C152 (1982)
Weight, $W$ (lbf)	1580	1670
Airspeed $V_E$ (kt)	67	67
Mean Height - sHp (ft)	2,600	2,500
Flaps, $\delta_f$ (deg)	0	0
Elevator Trim, $\delta_{t_{trim}}$ (deg)	10	10
Power (% BHP.)	56	66
Wing Loading $w$ (lbf/ft <sup>2</sup> )	9.91	10.47
CG aft of datum (inches)	35.69	33.56
CG as a percentage of CG range (%)	69.8	46.6
CG, 2 POB @ TOW, $h$ (%MAC)	27.00	23.39%
Estimated Elevator Gearing, $G$ (rad/ft)	1.39	1.50
Estimated downwash at tail, $\varepsilon$ (deg)	2.190	2.088
Estimated Downwash Derivative, $\frac{d\varepsilon}{d\alpha}$	0.4464	0.4464

## REFERENCES

---

- 1 European Aviation Safety Agency, Certification Specifications for Certification Specifications for Sailplanes and Powered Sailplanes, CS-22, Amendment 2, 5 March, 2009.
- 2 European Aviation Safety Agency, Certification Specifications for Large Aeroplanes, CS-25, Amendment 9, 25 August, 2009.
- 3 Federal Aviation Administration, Federal Airworthiness Requirements for Transport Category Airplanes, FAR-25
- 4 European Aviation Safety Agency, Certification Specifications for Normal, Utility, Aerobatic and Commuter Aeroplanes, CS-23, Amendment 2, 28 September, 2010.
- 5 Federal Aviation Administration, Airworthiness Standards: Normal, Utility, Acrobatic, and Commuter Category Airplanes, FAR-23.
- 6 Ministry of Defence, Design and Airworthiness Requirements For Service Aircraft Part 1 – Fixed Wing Section 2, Defence Standard 00-970 Part 1 Issue 5, 31 January, 2007.
- 7 US Department of Defence, Military Specification, Flying Qualities of Piloted Airplanes, MIL Spec 8785C, US DOD, 5 November, 1980.
- 8 Department of Defense, Handbook Flying Qualities of Piloted Aircraft, MIL-HDBK-1797, 19 December 1997.
- 9 Civil Aviation Authority, British Civil Airworthiness Requirements, CAP 482 Section S , Small Light Aeroplanes, Issue 5, 21 October, 2009.
- 10 Civil Aviation Authority, British Civil Airworthiness Requirements, CAP 467 Section K , Light Aeroplanes, Issue 7, 23 October, 1992.
- 11 European Aviation Safety Agency, Certification Specifications for Very Light Aeroplanes, CS-VLA, Amendment 1, 5 March, 2009.
- 12 Etkin, B., & Reid L.D., Dynamics of Flight – Stability & Control, 3rd Edition, John Wiley & Sons, Inc.1996.
- 13 Stinton, D., Flying Qualities and Flight Testing of the Aeroplane, Blackwell Science Ltd., 1996.
- 14 Smetana, F.O., et al, Riding and Handling Qualities of Light Aeroplane – A Review and Analysis, NASA Contractor Report CR -1975, March 1972.
- 15 Mathworks, MATLAB R2007a User Manual, Mathworks, 2007.
- 16 Leisher, L.L., & Walter, H.L., Stability Derivatives of Cessna Aircraft, Report Number 1356, Cessna Aircraft Company, Wichita, 1956.
- 17 Hoak, D.E, et al, USAF Stability and Control Datcom, Flight Control Division, Air Force Flight Dynamics, Laboratory, WPAFB, Ohio, 1978, revised.
- 18 Perkins, D.C., & Hage, R.E., Airplane Performance Stability and Control, John Wiley & Sons, New York, September, 1949.
- 19 Clarke, Bill, The Cessna 150& 152, 2nd Edition, TAB Books, 1993.
- 20 Cessna Aeroplane Corporation, Spin Characteristics of Cessna Models 150, A150, 152, A152, 172, R172, 177, Cessna Publications, August 1981.
- 21 Appareo, Appareo AS Flight Recorder GAU 1000 General Specification, Fargo, ND, US, June 2008.

- 
- 22 Bromfield, M.A., & Gratton, G.B., Supporting the investigation of factors affecting loss of control of light aeroplane, Proceedings of the 40th Annual International Symposium - Society of Flight Test Engineers, Sweden, September 2009.
  - 23 Roskam, J., Airplane Flight Dynamics and Automatic Flight Controls – Part 1, DARCorporation, Kansas, 2007.
  - 24 Cessna Aircraft Company, Cessna Model 150M, Pilots Operating Handbook, Cessna Publications, 1975.
  - 25 Cessna Aircraft Company, 1982 Model 152 Information Manual, Reprint, Cessna Publications 31 March 1983.